

EPIC: Abstraction and Polymorphism of In-Network Collectives on Ethernet

Yitao Yuan¹, Jianglong Nie¹, Tianyu Bai¹, Ruizhe Zhou¹, Siyuan Cao¹, Xujie Fan¹,
 Yuchen Xu¹, Junkai Chen¹, Chenqi Zhao¹, Nengyuan Zhang¹, Shaoke Fang¹,
 Jiangyuan Chen², Yuanfeng Chen³, Jiaqi Sun¹, Zhan Wang⁴, Xiaohua Xu²,
 Yuchao Zhang⁵, Yang Liu⁵, Xiangrui Yang³, Jing Lin⁶, Xiaohe Hu⁶, Yang Li⁷,
 Chao Jiang⁷, Limin Xiao⁷, Weifeng Zhang⁷, Junjie Wang⁸, Wei Cheng⁸, Yazhu Lan⁹,
 Jianbo Dong⁹, Binzhang Fu⁹, Wenfei Wu¹*

1 PKU, 2 USTC, 3 NUDT, 4 ICT, CAS, 5 BUPT, 6 Infracore, 7 Lenovo Research, 8 Centec, 9 Alibaba Cloud
 ETH+ Consortium

ABSTRACT

In-Network Collective (INC) acceleration holds immense potential for optimizing AI training and inference; however, its cross-layer nature has historically hindered investment and adoption within the open Ethernet ecosystem. To bridge this gap, we propose EPIC (Ethernet Polymorphic In-network Collective), an INC protocol specification and reference system built on the principle of “Unified Abstraction, Polymorphic Realization.” EPIC introduces an abstraction compatible with standard Ethernet that aligns functional boundaries with participant roles, while offering polymorphic realizations tailored to varying hardware capabilities.

We address three fundamental challenges: first, we employ a modular design that enables an evolutionary path from simple to complex implementations, allowing vendors to iterate their hardware incrementally; second, we apply formal verification methodologies to prove the correctness of all proposed polymorphic modes; and third, we develop a unified resource management model versatile enough for diverse INC scenarios. Extensive validation—spanning model checking, packet/flow simulations, VM emulation, Tofino Testbed, and FPGA/RTL verification—confirms EPIC’s correctness, performance gain, and feasibility.

This paper does not raise any ethical issues.

1 INTRODUCTION

As processing power for large-scale ML model training surges, communication overhead has become a critical performance impactor [6, 10, 24, 41, 41, 64, 73]. *In-Network Collective (INC)* communication, a new network communication paradigm, addresses this by offloading collective operations like AllReduce to switches, thereby compressing traffic, reducing trans-

mission time, and lowering overhead [25–27]. This efficacy has been proven by products such as NVIDIA SHARP [20, 21] and various prototypes [5, 40, 50, 64]. The open *Ethernet* ecosystem, one of the most mature and widely deployed networks [2, 17, 18, 51, 60, 61], is evolving into networking AI clusters and integrating INC capabilities.

Enabling INC within the open Ethernet ecosystem faces a core challenge: *single participants struggle to implement cross-layer INC systems independently*. Building INC requires the joint design of communication libraries, stacks, NICs, switches, and controllers, which are developed by different vendors and operators. The system’s integrity relies heavily on the interoperability of these components. This fragmentation poses two major risks for single participants, particularly switch vendors. First, isolated efforts within each scope fail to yield system-level benefits without corresponding host support, resulting in wasted investment. Second, the complexity of INC necessitates excessive upfront investment and prolonged coordination, potentially causing features to be shelved due to their impact on existing chip functions.

As a protocol standardization working group, we propose EPIC (Ethernet Polymorphic In-network Collectives), an INC protocol leveraging “**unified abstraction, polymorphic realization**” as a viable path forward on Ethernet. **(i)** It establishes a unified abstraction defining INC behaviors, participant functional scopes, and rigorous interoperability interfaces, while retaining implementation flexibility within each scope (§3). **(ii)** EPIC’s data plane aligns components with ecosystem roles via strict semantics, and we also propose three-mode polymorphic realizations (§4). **(iii)** EPIC’s control plane operates via software-defined networking (SDN), where a central controller manages global resources, policies, and rule dissemination (§6). EPIC addresses three critical challenges: the prohibitive development overhead for vendors to support various polymorphic realizations, the

*Wenfei Wu is the corresponding author; contact him by wenfeiwu@pku.edu.cn. Authors are also members of ETH+ Consortium.

Table 1: Implementations and Key Results

Implementation	Target Property	Key Results
Model Checking	Correctness	All 3 modes are correct.
Tofino Testbed	Performance Acceleration	Up to 1.59x for collectives and 1.35x for training.
Emulation	Interoperability, Evolvability	All 3 modes work with RoCE. Mode-III reuses 61% of Mode-II.
Flow-level Simulation	Gain in Resource Management	Reduce GPT-3 JCT by up 45.8%, multi-job 99%-tile JCT by 30.9%
Packet-level Simulation	Loss Tolerance	Mode-III outperforms Mode-II.
FPGA	Latency, Resource Cost	50 ns processing latency O(1) MB SRAM
RTL	Chip Feasibility	3.2 Tbps; 4.89 mm ² @ 28 nm

complexity of verifying protocol correctness across these modes, and the lack of a unified resource model to support various management policies (§2.3).

EPIC protocol specification was distributed to multiple organizations for comprehensive validation. The protocol working group members make various implementations and validate EPIC’s properties as in Table 1.

In this paper, our contributions are as follows.

- A unified abstraction of six-primitive collectives to enable INC systems in Ethernet ecosystem,
- A polymorphic data plane enabling the switch manufacture for vendors with diverse capabilities,
- Modularized data plane enabling switch vendors to evolve INC switch between polymorphic modes,
- Analysis of properties of polymorphic modes, including model-checking verified correctness, transmission efficiency, space complexity, logic complexity, and fault tolerance,
- Resource model derived from the abstraction that enables various resource management policies.

2 BACKGROUND

2.1 EPIC’s Application Scope and Benefits

EPIC focuses on scale-out networks. AI clusters use dual-interconnects: scale-out (NIC/switch-based) and scale-up (e.g., NVLink [55], UALink [69]). EPIC targets the Ethernet/RoCE ecosystem [30, 42] for scale-out expansion, embedding INC semantics in RoCE header fields, which is the de facto standard on Ethernet [2, 18]. This avoids the fragmentation of scale-up protocols and the prohibitive hardware barrier of redesigning accelerator IO dies for new protocol layers, ensuring multi-vendor interoperability.

EPIC focuses on regular collectives. We distinguish primitives by data patterns: **(1) Regular:** AllReduce, Reduce, and Broadcast. These maintain strict alignment between element indices, packet sequences, and memory addresses. **(2) Irregular:** MoE token dispatch/combine (AlltoAllv)[49]. These involve asymmetric traffic and lack positional correspondence. Designing for irregular patterns requires complex index-to-memory mapping and congestion management. Its

numerous dispatch/combine traffic patterns also challenge the forward table volume if implemented using IP multicast and EPIC’s lookup table. We have another design for MoE AlltoAllv, which will be released separately.

EPIC benefits communication and end-to-end model training/inference. INC enhances communication by reducing latency (fewer hops), minimizing traffic congestion, and lowering end-host overhead to better saturate bandwidth. For end-to-end tasks, INC provides direct acceleration in communication-bound clusters. In optimized environments, it still yields substantial gains for expensive hardware by freeing GPU resources for computation, raising the performance floor, and simplifying system tuning.

2.2 Requirements of INC on Ethernet

EPIC should satisfy requirements from ecosystem organization, hardware-offloading trend, and AI collective patterns.

(1) EPIC must strictly adhere to Ethernet functional scopes and interoperability. It partitions components according to the industry division of labor, where functionality results from collaboration between CCL developers, NIC/switch vendors, and operators via standard protocols like IP and RoCE. Standardizing these interaction primitives is essential to avoid the risks of closed, vertically integrated solutions. By defining clear interoperability specifications, EPIC enables cross-layer optimization without sacrificing vendor neutrality. This alignment is a prerequisite for breaking ecosystem deadlock and enabling deployable INC.

(2) EPIC must strictly align with RoCE, one of the de facto standards for AI interconnects [17]. As bandwidth scales toward 1.6 Tbps, hardware transport offload via RoCE is essential to bypass the CPU “performance wall” and maintain zero-copy, low-latency transfers. Unlike previous software-based INC (e.g., SwitchML¹ or ATP), EPIC leverages mature hardware-offloaded engines to sustain line-rate speeds. This approach treats INC as an enhancement of existing infrastructure rather than a replacement. By inheriting RoCE’s congestion control and memory semantics, EPIC enables vendors to scale bandwidth without the cost of proprietary protocols, ensuring a production-ready and evolvable ecosystem.

(3) EPIC must support a comprehensive suite of collective primitives beyond AllReduce. To keep pace with evolving AI workloads—such as FSDP (ZeRO) [62, 82], which relies on ReduceScatter and AllGather—a modern INC framework must offer versatile support for diverse patterns, including Broadcast and Reduce. Exhaustive primitive support is critical for deployment viability. Broad functional coverage eliminates the need for hybrid deployments, where missing hardware-offloaded primitives force a mix of INC

¹SwitchML is developed on DPDK or RDMA UC.

and conventional CCLs. By avoiding such fragmentation and its associated orchestration overhead, EPIC serves as a general-purpose accelerator. This ensures a consistent, high-performance communication fabric that is both future-proof and production-ready for AI training and inference.

2.3 Challenges

We overcome the challenges of ensuring evolvability and correctness in a polymorphic data plane while maintaining control plane generality.

(1) Diverse performance-complexity tradeoffs (§5) and high development overhead hinder universal polymorphic INC support. In the Ethernet ecosystem, switch capabilities vary: fixed-function ASICs prioritize throughput over flexibility, while programmable targets (e.g., Tofino[31]) are limited by SRAM and ALU resources. This disparity forces vendors to choose between costly full-spectrum implementation or restrictive single-mode solutions.

To resolve this, EPIC *modularizes switch INC functionality*, enabling a low-cost transition from simple to complex modes. By decoupling functionalities into reusable components, vendors achieve scaling through module composition. This adaptive approach allows implementations to align with specific hardware constraints—from basic packet replication to full RoCE endpoints—facilitating an incremental and sustainable deployment path for the industry (§4).

(2) Polymorphic realizations complicate the verification of computational integrity. Ensuring protocol termination and server-equivalent results is challenging, as each mode introduces unique intermediate states and cross-layer interactions. Analyzing these diverse designs individually incurs prohibitive analytical overhead.

To address this, we performed a *formal analysis* of the EPIC protocol suite. Using automated model checking, we systematically explored the state space of the polymorphic data plane and network conditions (e.g., packet loss). This rigorous approach automatically verifies protocol termination and computational accuracy across all modes, providing provable guarantees of system integrity while eliminating manual, error-prone proofs (§5).

(3) Distributed switch resources lack a unified model to support diverse, scenario-specific management policies. The increasing heterogeneity of AI workloads—ranging from multi-tenant environments to varied cluster scales—demands unique allocation strategies. Manually coordinating customized INC management for every infrastructure combination is infeasible due to extreme complexity.

To bridge this gap, we propose a *unified INC resource model* based on the SDN paradigm. By virtualizing switch resources and decoupling the control from the data plane, this model provides generic interfaces for centralized orchestration. This architecture supports diverse policies—including

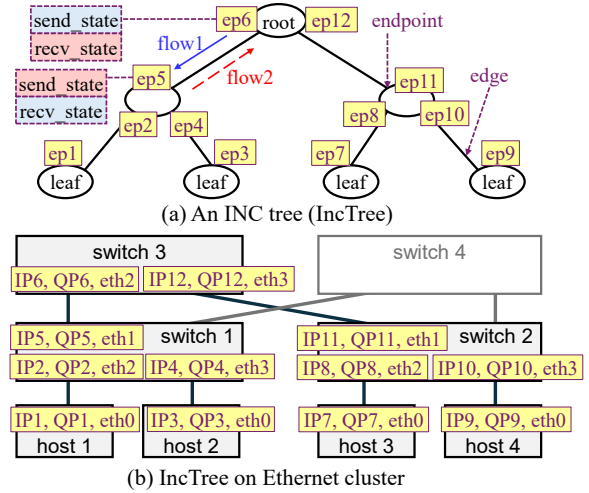


Figure 1: EPIC’s abstraction

isolation and contention-based sharing—transforming fragmented resources into a flexible, programmable fabric. This approach minimizes administrative overhead while maximizing resource utilization across dynamic AI scenarios (§6).

3 EPIC OVERVIEW

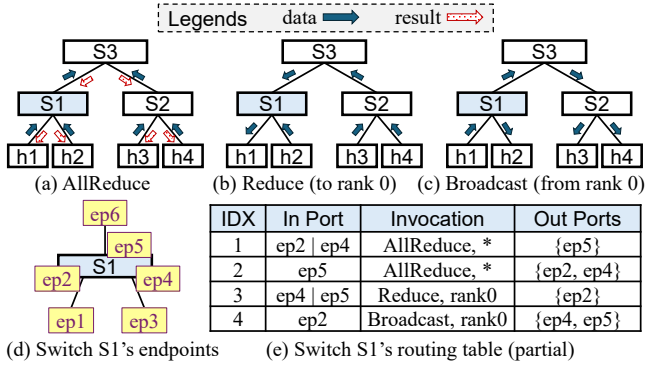
3.1 Abstraction

We define EPIC’s abstraction and map it to Ethernet clusters. EPIC’s realization can support 6 collective primitives.

INC Tree. Collective communication is performed on a group of parallel application processes, called *ranks*. EPIC employs an *INC Tree (IncTree)* to describe the logical topology of a communication group (Figure 1). Each rank maps to a leaf node, while non-leaf nodes act as intermediate aggregation or replication points within the network fabric. The tree is assigned a *root*. An *edge* connects two nodes on the tree, and is undirected. Data unit (packets) on an edge with the same direction form a *flow*.

We define an *endpoint* to describe flow routing and transmission. An edge has two *endpoints*, each on one of the edge’s two nodes. Note that a node can connect to multiple edges, but those edges’ endpoints on that node are distinct. On an edge, a flow’s *transmission states* consist of sending states on its source endpoint and receiving states on its sink endpoint (Figure 1a). In a node, a flow’s *routing* from one edge to another can be described as from one endpoint to another.

Collectives on IncTree. EPIC performs various collective primitives on the aggregation tree. It supports six primitives: AllReduce, Reduce, Broadcast, Barrier, ReduceScatter, and AllGather. The latter three can be derived from the former three (Figure 2a to Figure 2c): Barrier is equivalent to an AllReduce with an empty data payload, ReduceScatter is the sequential execution of multiple Reduces, and AllGather is similarly the execution of multiple Broadcasts (Appen-


Figure 2: Data Flow and Routing in IncTree

dix §A). Thus, in the following text, we focus on the design of AllReduce, Reduce, and Broadcast.

IncTree on Ethernet Cluster. In Ethernet-based Clos topologies, hosts reside at the edge while switches form the core. An IncTree maps leaf nodes to hosts and intermediate nodes to switches. Each endpoint is defined as an $\langle \text{IP}, \text{QP} \rangle$ tuple associated with a specific host NIC or switch port (Figure 1b). Consequently, an IncTree edge may span multiple physical links defined by the path between its two endpoints. The IncTree abstraction also applies to accelerator-centric topologies [33], with non-leaf nodes on accelerators.

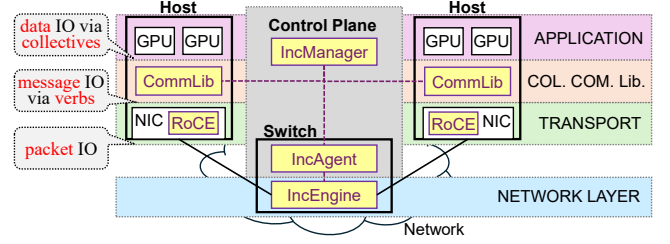
During collectives, switches execute local actions via match-action tables. These tables recognize and forward packets to ports that align with the IncTree’s data flow. For instance, in an AllReduce operation (Figure 2e), switch S_2 aggregates packets from child endpoints (ep_8, ep_{10}) toward the parent (ep_{11}) and distributes results back down those same paths.

3.2 Architecture

Architecture. EPIC decouples control and data planes, aligning with industry functional boundaries. The data plane comprises host-side *CommLib*, standard NIC *RoCE*, and switch-based *IncEngine*. The control plane features switch-resident *IncAgents* and a centralized *IncManager* for resource discovery, policy formulation, and rule dissemination (Figure 3).

Interfaces. Components interact through standardized interfaces across two paths: (1) **Control Path:** The *IncManager* coordinates with *CommLib* and *IncAgent* via RPC. The *IncAgent* then configures the *IncEngine* using internal register or table updates; (2) **Data Path:** A layered collaboration ensures interoperability.

The data path consists of three components. (1) *CommLib*: Provides collective primitives (e.g., AllReduce) to applications and exchanges data with the NIC via standard RDMA Verbs. (2) *RoCE*: Executes standard RDMA operations without hardware changes, interfacing with the *IncEngine* via *RoCE* packets over physical links. (3) *IncEngine*: Performs packet-level parsing, processing (aggregation/replication), and forwarding between NICs or peer engines.


Figure 3: EPIC Architecture

3.3 Workflow

3.3.1 System and Group Lifecycle

Bootup. The lifecycle begins with component initialization: *CommLib* daemons launch on hosts, and *IncEngine* is enabled on switches. All instances report local states to the *IncManager*, which constructs the global topology and manages resources (§6.1).

When an application calls *InitGroup()*, the *IncManager* computes and maps a logical IncTree onto the physical fabric. It then disseminates configurations: host *CommLib*s receive flow information, and switch *IncAgents* install local routing states into their respective *IncEngines*.

Connection and Routing. Following the setup, *CommLib* establishes *RoCE* connections to neighbor switch nodes. Switches support polymorphic connection handling, ranging from full stack functionality to state-less translation (§4.2, §4.3, §4.4). During initialization, *IncManager* pre-computes rules for all $2N + 1$ traffic patterns (AllReduce, Reduce, Broadcast) and configures forwarding for both *RoCE* data and ACK packets.

Teardown. Upon completion, *DestroyGroup()* triggers the *IncManager* to instruct *IncAgents* to delete local states and forwarding rules. The *IncManager* then releases group-specific resource reservations for future allocation.

3.3.2 Runtime Collective Invocation

Control Signaling. EPIC supports multiple runtime primitives using in-band signaling, avoiding the custom INC headers like SHARP or the CPU-intensive header prepending like NetReduce. Before data transmission, the *CommLib* sends a standalone RDMA Send with Immediate message² to notify IncTree nodes of the collective type, root, and data size. This signaling is pipelined with subsequent data to hide latency. If lost, the switch refuses data processing until retransmission, ensuring protocol safety through validated PSN range (derived from the data size).

Data Processing. The execution follows a five-step pipeline: (1) **Chunking & Flow Control:** *CommLib* partitions tensors into messages and applies application-level flow control to prevent switch buffer overflow. (2) **Standard Transport:** The commodity NIC encapsulates messages into *RoCE* packets for delivery to the *IncEngine*. (3) **Switch Processing:** The In-

²Send With Immediate has a distinct *RoCE* OP Code from other verbs.

cEngine performs aggregation, replication, or forwarding. It identifies the collective setting via the preceding control message and uses pre-configured rules to route packets through the IncTree. (4) Reliable Reception: Receiver NICs reassemble packets and signal CommLib via Work Completions (WC). RoCE ACK/NAK packets are processed by the IncEngine on the reverse path to manage state release (§4). (5) Completion: CommLib assembles the results and returns control to the application.

3.4 System Fault Tolerance.

Running distributed training with EPIC needs to handle runtime failures from switches, links, and/or ranks. EPIC can run as a network slice (separate CommLib and IncEngine instances from traditional CCL and switch forwarding), and set up NCCL as failover; the failover process can be enabled via services like MCCS [75].

EPIC itself handles failures by reinitializing groups [70]. System-level failover requires sandboxing ranks and runtime group member change; EPIC can apply Continuum [39].

4 POLYMORPHIC DATA PLANE

EPIC modularizes IncEngine; composing modules in different ways forms different modes, and reusing modules evolves modes from simple to complex.

4.1 Modularize IncEngine

We decouple the runtime communication group states from the processing logic, and decompose all functionalities in IncEngine into independent modules. At runtime, these modules retrieve the corresponding states using the header of the current packet, and execute specific logic.

States and Context. The collection of all states involved in an INC group at runtime is referred to as the group’s *Context*. While an INC group logically possesses a global context across the entire cluster, physically, each switch is only required to install the *Local Context* relevant to its operation; where there is no ambiguity, we use “context” to refer to “switch local context”.

On an IncTree switch node, the states include: (1) routing states, in the format of rules to look up packet headers and decide the output ports, (2) transmission states, where each endpoint involves sending states for its outgoing flow and receiving states for its incoming flow, and (3) computation states, which are buffers to temporally store intermediate states. At runtime, modules utilize the header of the current packet to retrieve its context. These three kinds of states are described and retrieved by the endpoint in the IncTree abstraction.

Function Modules. We prepare the following modules to construct IncEngine. There are modules for state retrieval and routing based on the packet header: `LookupTable`, `TranslateHeader`, and `Forward`. There are modules for flow

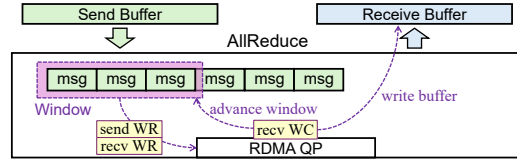


Figure 4: Flow Control in CommLib

Table 2: Symbols and meaning

U : Maximum Transmission Unit (MTU); unit is byte	
M : message size; unit is MTU; a message is UM bytes	
W : window size; unit is message; a window is UMW bytes	
N : array size in IncTree state	
H : aggregation tree depth	D : node degree
B : link bandwidth	L : link latency

transmission: ReceiveAck, SendAck, and Retransmission. There are modules for data (packet payload) operation: CheckDuplicate, AggregateData, RecycleBuffer, and ReplicateData. Module internal logic is elaborated in Algorithm 1 and 2 in Appendix B.

4.2 Mode-I: Connection Terminated

Mode-I provides a “heavyweight” realization of the EPIC abstraction for high-end switches capable of supporting a full RoCE stack. In this mode, the switch functions as a Parameter Server (PS), terminating host connections and maintaining complete transport states to ensure reliable transmission. The architecture utilizes a layered protocol stack where the switch handles deduplication, ACK processing, and message reassembly.

AllReduce workflow. The host-side CommLib initiates communication with the control signal. To manage traffic, the system employs message-granularity flow control using paired Send-Recv verbs. This choice is critical as one-sided Write verbs that do not provide work completion (WC) signals that confirm “result” readiness. Flow control is achieved by setting the RoCE outstanding WR to be W messages, where W is configured as a system parameter window size (Figure 4).

Intermediate switches identify EPIC packets via lookup tables, directing data to internal transport layers for hop-by-hop reliable delivery, and to the internal application layer for data aggregation (performed by the AggregateData module). Once the IncTree root completes data reduction, the ReplicateData module broadcasts results back to child nodes via the transport layer again; the child nodes relay the results towards host receivers (Figure 5a).

Reduce and Broadcast workflows. They serve as simplified variations of this process. In a Reduce operation, data flows unidirectionally from multiple senders to a single receiver through switch-based aggregation, with host CommLibs executing only Send or Recv verbs, respectively. Conversely, Broadcast transmits data from one sender to multiple receivers using the replication module. Both primitives lever-

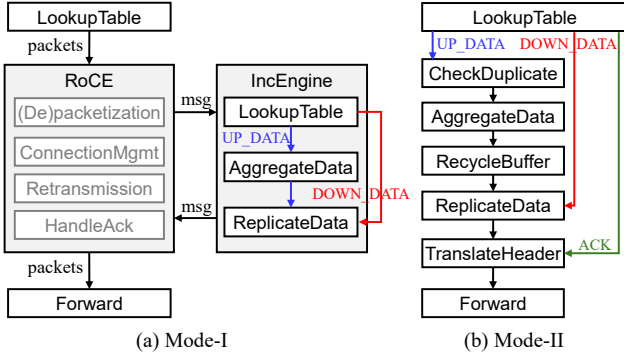


Figure 5: Modules and data flow in three modes

age the same pre-configured routing rules and polymorphic RoCE functions, ensuring high-performance communication without the bidirectional result distribution required by AllReduce.

Interaction with RoCE Flow Control and Congestion Control. EPIC’s flow control means keeping inflight data volume from overwhelming the switch buffers. The three mechanisms – EPIC flow control, RoCE congestion control, and RoCE flow control (e.g., PFC or CBFC) – are layered in the order above, and they work independently. The actual runtime traffic rate, progress, and volume are the minimum of the three mechanisms. Such independence of EPIC flow control from RoCE congestion control and flow control holds for all three modes.

4.3 Mode-II: Connection Translated

Mode-II offers a minimalist design for switch vendors by substituting full transport termination with a “connection translation” approach. Instead of maintaining complete RoCE states, the switch modifies and forwards packets while relying on end-hosts for reliability, ensuring transport transparency. This mode requires all NIC endpoints to be initialized with identical Packet Sequence Numbers (PSNs).³

AllReduce Workflow. (1) CommLib works in the same way as mode-I. The switch maintains a payload (array of MTU) buffer and a degree buffer (array of counters), both of size N .

(2) The switch identifies upward data packets by header fields (Figure 7f), and processes them by modules. CheckDuplicate identifies retransmissions. For the first arrival of a packet, AggregateData module sums up its payload into payload buffer (at $idx = pkt.psn \% N$)⁴ and increments the degree at idx ; for retransmission, aggregation is skipped. If aggregation is incomplete ($degree[idx] < FAN-IN$), the packet is dropped; otherwise, the result ($payload[idx]$) is copied back to the packet, forming a *result packet*. ReplicateData fur-

³PSN can be set through `ibv_modify_qp()`.

⁴If reproducibility is needed (adding numbers in a deterministic order) [7, 72], IncEngine needs extra buffers to store data first, and add data up when the degree is full.

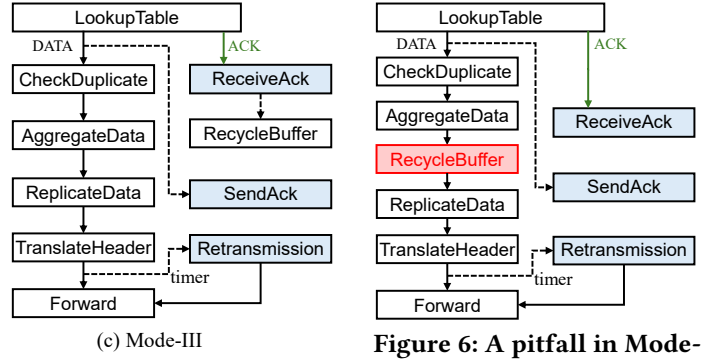


Figure 6: A pitfall in Mode-III design

ther determines the next hops, and TranslateHeader clones the packet and modifies header fields (e.g., Dest IP, Dest QP). Finally, Forward sends the packet to corresponding switch port.⁵

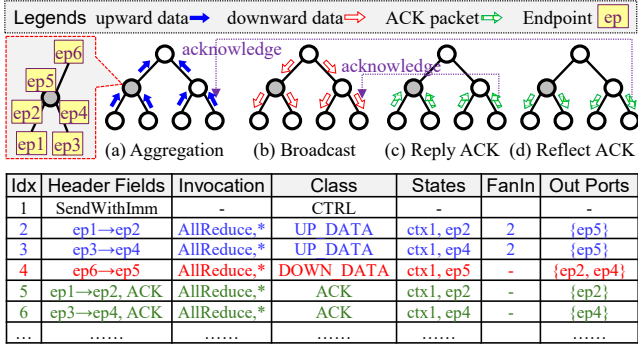
RecycleBuffer: The *payload/degree* size is set to twice the window ($2MW$ MTUs). To support streaming with minimum switch SRAM space, *payload* is used circularly: upon completion of aggregation ($degree[idx] == FAN-IN$), the slot at $(psn + MW) \% (2MW)$ is cleared for subsequent packets; this is a safe operation as that slot is out of all senders’ windows [50, 80].

(3) The IncTree root sends result packets downward. Switches identify downstream packets (Figure 7b, Figure 7f) and process them via ReplicateData, TranslateHeader, and Forward modules (Figure 5).

(4) The result packet finally reaches the RoCE NIC, and triggers an ACK (Figure 7c). This ACK is reflected by the first-hop switch back to the RoCE NIC to acknowledge the upstream data packet (Figure 7d). RoCE ACKs are cumulative, and this mechanism ensures correctness even if ACKs are coalesced. Negative ACKs (NAKs) generated due to packet loss are handled in the same way as ACKs: reflected to trigger standard RoCE retransmission at the sender. In the case of packet transmission, each step of the workflow is idempotent (repeatable without affecting the result).

Reduce and Broadcast Workflows. (1) Reduce: Control and data packets are handled the same as AllReduce; the receiver’s RoCE NIC replies ACKs, which are broadcasted along the tree to the senders. NAKs are handled similarly. (2) Broadcast: Control and data packets are sent to receivers along the IncTree, replicated at each node. Receivers reply with ACKs towards the sender, which are aggregated by IncTree nodes. ACKs are cumulative; intermediate nodes maintain an *ackPsn* for each endpoint to record the progress of cumulative ACK. A node also records a *nodeAckPsn* as the

⁵The endpoint states also include RDMA memory_region (MR) address and rkey to enable the write admission to the RDMA registered memory region. address and rkey are distributed (from host CommLib to switch IncEngine via IncManager) during group initialization.



(e) The highlighted switch’s lookup tables (AllReduce entries)

Figure 7: Lookups tables in Mode-II

minimum of all child *ackPsn* values. An ACK is forwarded upstream only if it updates the *nodeAckPsn*, effectively preventing ACK amplification. NAKs caused by packet loss are not aggregated but are forwarded to the sender to trigger retransmission [28, 43].

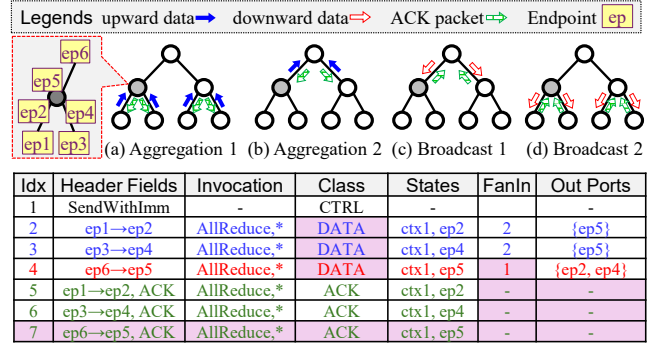
Group PSN Synchronization. A primary challenge in multi-collective support is PSN divergence, where asymmetric primitives like Reduce or Broadcast cause sequence numbers to drift between ranks, breaking subsequent AllReduce alignment. A “work-around” method for this issue is to mandate single-primitive groups and use multiple subgroups for complex operations like ReduceScatter. This method increases the lookup table entries: an *N*-member group needs to configure $2N + 1$ EPIC groups, *N* for reduce, *N* for broadcast, and 1 for AllReduce. Considering a switch only holds a few local groups and *N*’s scale, the table entry cost is acceptable. The switch memory is temporally multiplexed among collective invocations.

We also suggest a “RoCE-Refined” approach: allowing a northbound NIC interface to manually synchronize sequence numbers after asymmetric operations. This architectural flexibility ensures that Mode-II functions correctly across diverse traffic patterns while minimizing switch hardware modification.

4.4 Mode-III: Connection Augmented

Mode-III serves as a middle ground between the full-stack complexity of Mode-I and the minimalist nature of Mode-II, providing hop-by-hop retransmission (Link-Level Retry, LLR) without the overhead of complete message packetization (Figure 8).

A Pipe Abstraction. This mode introduces a *pipe* abstraction to manage buffer readiness and transport reliability at each switch hop (Figure 9). Each pipe consists of a payload buffer and a degree buffer—both sized *N*—and maintains a *psnStart* value representing the valid PSN range [*psnStart*, *psnStart*+*N*). A pipe is associated with one or several incoming endpoints (whose count is the FAN-IN degree) and one or several outgoing endpoints.



(e) The highlighted switch’s lookup tables (changes with Mode-II highlighted)

Figure 8: Lookups Tables in Mode-III

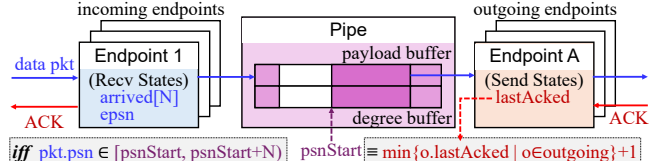


Figure 9: The Pipe Abstraction.

When an incoming endpoint receives a data packet, it performs a readiness check: if the PSN falls within the valid range, the *AggregateData* module processes the payload and immediately generates an ACK to the upstream node; otherwise, the packet is dropped, and a NAK is sent to trigger retransmission or congestion control. If the packet is processed and the degree is full, the switch sends the packet further to downstream endpoints (via *ReplicateData* and *TranslateHeader*).

When an outgoing endpoint receives an ACK, the endpoint maintains and updates a *lastAcked* state, which is the maximum ACK PSN it observed. This value is used to dynamically update the pipe’s *psnStart* (defined as the minimum of all outgoing endpoints’ *lastAcked* + 1), thereby advancing the sliding window and freeing buffer space for subsequent packets (Algorithm 2 in Appendix §B).

AllReduce Workflow. (1) *CommLib* and RoCE NIC remain consistent with Mode-I/II. (2) Upward data packets are handled by an aggregation pipe, with multiple incoming endpoints and one outgoing endpoint. (3) Downward packets are handled similarly by a broadcast pipe, with one incoming endpoint and multiple outgoing endpoints. (4) RoCE NIC sends NAKs when observing packet loss, and switch handles NAK by retransmitting packets starting from *lastAcked* + 1. Whether a switch actively sends NAK when it observes packet loss (e.g., out-of-order) is optional, both choices work correctly, but sending NAK is recommended for performance issue (Appendix H.4).

Reduce and Broadcast work with one pipe on each switch, enabling one-direction data flow.

Group PSN Synchronization. *IncTree* edges allow bidirec-

tional transmission; unidirectional operations (Reduce/Broadcast) desynchronize the sequence numbers of the reverse flow on the same edge. To resolve this in Mode-III, when an ACK for a flow in one direction arrives at an endpoint, the system must simultaneously update the PSN progress of the reverse flow (i.e., $ePSN$) on that endpoint to match the group progress. We leave the discussion of other possible modes and switch microarchitectures in the appendices §D and §E.

Congestion Control for Rate Synchronization. In Mode-III, rank windows progress independently. If ranks experience different congestion conditions, the congested ranks progress slowly while the uncongested ones progress quickly. It is a better choice to have the switch slow down the faster ranks to avoid excessive sending and dropping (due to being out of the pipe PSN range). On the first-hop switch, if a packet is dropped due to exceeding the PSN range, the switch replies to the sender with a congestion signal (e.g., CNP for DCQCN) to slow down that rank.

5 ANALYSIS OF MODES

5.1 Correctness

Analysis. The correctness of the EPIC protocol is established through two primary pillars: computational equivalence to single-node processing and guaranteed protocol termination.

In Mode-I, correctness is inherited from the underlying RoCE transport layer, which ensures that IncEngine only processes ordered, unique, and valid packets. This reliability allows the engine to index data structures directly by sequence number for inherently accurate aggregation.

For Mode-II, end-host retransmission ensures data completeness, while the CheckDuplicate module prevents redundant computation. Addressing conflicts are mitigated by the “aggregate-then-forward” mechanism, which constrains the skew between the fastest and slowest ranks. This ensures the PSN range of in-flight packets never exceeds twice the window size ($2W$). By sizing switch buffers to $2W$, we prevent packet collisions and incorrect buffer mapping.

Mode-III similarly utilizes hop-by-hop retransmissions and redundancy detection. Here, each computation buffer maintains a strict permissible PSN range exactly matching its capacity (N). This prevents addressing conflicts where packets with a PSN difference greater than N might otherwise alias to the same memory location.

Across all modes, a robust timeout-retransmission failsafe guarantees eventual protocol termination under any network condition.

Model Checking. The correctness of EPIC is verified via formal model checking, where each network node is modeled as a Non-deterministic Finite Automaton (NFA). State transitions are triggered by packet processing, and non-determinism arises from the concurrent nature of multi-port

reception and transmission.

The global protocol state is represented by the composition of these individual NFAs into a unified, complex system. To verify the protocol, the model checker exhaustively simulates all execution branches from every state, accounting for network uncertainties such as packet loss and out-of-order delivery. For each transmitted packet, the checker explores every possible outcome—success, loss, or reordering—creating separate execution paths for each scenario.

The protocol is deemed correct only if every explored branch satisfies two invariant properties: computational accuracy (the final result matches server-side reduction) and liveness (the protocol eventually reaches a terminal state). This rigorous exploration of the state space ensures that the polymorphic data plane remains robust under any possible network condition.

The EPIC model checker provides a specification language to describe an INC system, including topology and node logic, and a compiler to compile a user program to a TLA+ program; it runs TLA+ model checker to verify the system correctness.

The EPIC model checker overcomes two challenges. First, it enables describing network nondeterminisms including reliable, unreliable, and out-of-order packet delivery. Second, it handles state explosion by input space reduction, nondeterminism constraints, and symmetric state elimination.

Fixing a Pitfall. Model checking revealed a critical pitfall when evolving from Mode-II to Mode-III regarding buffer management. In Mode-II, buffer slots out of the current window are recycled when an aggregation event occurs inside the current window, as the “aggregate-then-forward” mechanism naturally synchronizes window advancement across all ranks (RecycleBuffer in §4.3).

However, direct application of this logic to Mode-III is incorrect (Figure 6). In Mode-III, window progression is independently governed by ACKs, meaning that the completion of an aggregation at a specific PSN does not guarantee that the $PSN + MW$ position is outside the active windows of all participants. Clearing the buffer at $PSN + MW$ prematurely risks erasing data from faster ranks, resulting in computational corruption. To resolve this, we introduced the pipe abstraction (pipe in §4.4), which mandates a unified writable range to forcibly synchronize sender progress.

In addition, the EPIC model checker also finds design risks in ATP, SwitchML, and NetReduce. And we fix them in EPIC technical report. We put other insights in Appendix§H.

5.2 Other Properties

We compare other properties across three modes, and reach the following conclusion. Formal analysis is placed in the Appendix §F, and Figure 10 illustrates their comparison.

Transmission Efficiency. Switches operate under a store-and-forward model but at different granularities. Mode-I

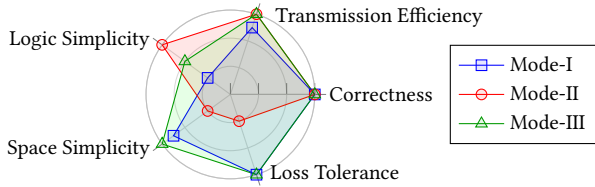


Figure 10: Comparison of Modes (outer is better).

requires full message reception prior to processing, whereas Mode-II/III utilize packet-level (MTU) pipelining. Consequently, Mode-II/III reduces end-to-end latency by approximately $(2H - 1)(M - 1)U/B$, offering advantages unless the message size S is exceptionally large or the propagation delay L dominates.

Logic Complexity. Considering the module organization, Mode-II is the simplest to implement, followed by Mode-III and Mode-I.

Space Complexity. Mode-II carries the highest space overhead $4(H - 1)BL$ because its end-to-end flow control must buffer for the entire path bandwidth-delay product (BDP). In contrast, Mode-I and Mode-III utilize hop-by-hop mechanisms, requiring only single-hop BDP buffers (non-reproducible $4BL$ to reproducible $(D + 1)2BL$). Mode-III achieves the best balance, offering lower space requirements than Mode-II while supporting non-reproducible options to further minimize overhead.

Loss Tolerance. Throughput in Mode-I and Mode-III scales with the slowest independent hop due to local retransmissions. Mode-II, however, suffers from multiplicative degradation because packet loss at any rank forces global synchronization and retransmission across the entire IncTree. While all modes perform similarly in lossless environments, Mode-I and Mode-III are significantly more robust to network noise.

6 INC RESOURCE MANAGEMENT

6.1 Resource Model

Architecture. The EPIC control plane enables intelligent resource management through a centralized IncManager and distributed IncAgents. During initialization, the IncManager constructs a global view by aggregating reported device capabilities, port statuses, and available on-chip SRAM from each IncAgent, while simultaneously performing global topology discovery via link-state reporting.

At runtime, the IncManager serves as the decision-making hub, instantiating communication groups by issuing instructions to IncAgents. These instructions configure the switch-local context, including lookup tables and computation states such as aggregation buffer offsets. By decoupling policy formulation from hardware execution, the framework supports dynamic resource reallocation and real-time state updates based on network conditions. This architecture ensures fine-grained, centralized control over distributed INC resources,

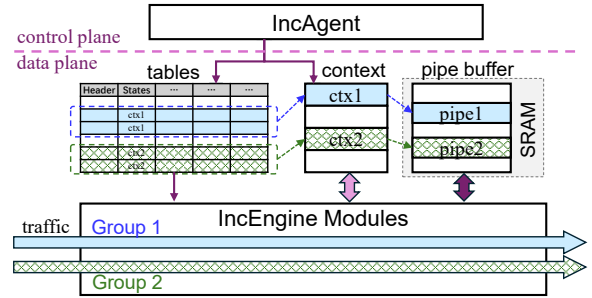


Figure 11: Resource model

maximizing efficiency across the cluster.

Indirection Layer for Resource Allocation. In the EPIC architecture, switches manage group-specific rules in match-action tables and associated contexts in high-speed SRAM. Direct context reallocation via table modification is computationally expensive due to the high volume of rules. Analysis reveals that most SRAM is consumed by transient states—such as payload and degree buffers ($O(\text{BDP})$)—which remain idle between collective invocations, while persistent endpoint states ($O(D)$) remain minimal.

To optimize utilization, EPIC introduces an indirection layer that decouples these large transient states from the fixed context. By utilizing pointers within the context to reference dynamic SRAM regions, the IncManager can calculate and assign memory offsets in real-time. This pointer-based approach facilitates agile, fine-grained resource reallocation and significantly enhances SRAM utilization without the overhead of reconfiguring global forwarding tables.

6.2 Supporting Various Policies

Cluster-wide INC resource management essentially needs to place an IncTree on the topology and decide the resource allocation on each of its switch nodes. EPIC resource model can support various existing and new policies, where we list three classes below.

Edge-Disjoint Tree. Legacy INC solutions often utilize an Edge-Disjoint Tree (EDT) approach [12, 63] necessitated by fixed-function hardware. These systems reuse static ingress buffers that cannot be virtualized, meaning a physical port can typically serve only one communication group. This creates a strict topological constraint: multiple aggregation trees must not share edges to avoid resource contention.

The EPIC resource model maintains compatibility with EDT by decoupling IncTree placement from resource allocation. EPIC first determines an EDT for a group and then independently allocates SRAM resources to bind the tree.

We provide an algorithm to calculate candidate EDTs within Clos networks. The process removes edges occupied by active EDTs, then iteratively scans switches from lower to upper tiers. It identifies the lowest level containing switches reachable by all group members without traversing higher

levels. The algorithm returns these switches as potential IncTree roots or indicates if no such candidate exists.

Spatial Multiplexing. Legacy solutions like SwitchML [64] and NetReduce [50] achieve isolation by statically partitioning switch SRAM, typically for single-tier scenarios. EPIC extends this to cluster-wide, multi-layer topologies, enabling non-interfering concurrent groups and robust multi-tenancy.

To manage this, EPIC jointly optimizes IncTree placement and resource allocation by evaluating both logical connectivity and “path width”—a metric combining available bandwidth and SRAM capacity. Notably, the system may prioritize longer paths if their larger aggregation buffers support superior congestion control and higher overall throughput.

For Clos networks, we employ a greedy iterative algorithm to identify the Pareto frontier of candidate IncTrees. By scanning from lower to upper levels, the algorithm identifies potential roots that balance tree depth against resource capacity. This provides administrators with a selection of optimal solutions, ranging from low-latency trees for synchronization to high-bandwidth trees for data-intensive training.

Temporal Multiplexing. To maximize efficiency, EPIC supports temporal resource sharing like ATP [40, 45, 46]. It models switch capacity as a combination of unallocated space and oversubscribed blocks weighted by duty cycle. This allows the IncManager to perform joint placement and allocation even in congested environments, effectively multiplexing physical SRAM across multiple communication groups.

Mutual exclusivity can be maintained primarily through scheduled coordination, which staggers group invocations. This is particularly effective for 3D parallel training, where Tensor Parallel (TP) and Data Parallel (DP) groups communicate in interleaved phases, enabling them to share physical hardware without contention.

In decentralized or multi-tenant scenarios where scheduling is infeasible, EPIC employs a contention-and-fallback mechanism. Groups attempt to “lock” resources via a first-come-first-served (FCFS) policy at switch-resident recorders. If a group fails to secure the complete IncTree, it performs an all-or-nothing release and falls back to host-based communication (e.g., NCCL), preventing partial occupancy and ensuring system-wide progress.

7 EVALUATION

7.1 Experiment Settings

Implementation. The EPIC standard specification is provided to the organizations in the working group, and the group contributes several different implementations, each of which can validate the specific attributes of EPIC as described in Table 1. The following implementations are anonymously open-sourced in the Appendix. Model checking is built in TLA+ [38], Tofino testbed prototype, OVS emulation [59]

connected VMs, flow simulation in OMNET++, packet simulation in NS3.

Environments. Our testbed has four servers and one switch in a star topology. Each server has two NVIDIA GeForce RTX 3090 GPUs, two Xeon(R) Silver 4316 CPUs with 40 physical cores, 192 GB memory, 1 TB SSD, two 100 GbE CX-5 NICs (each NIC bonded with a GPU); the switch has 100 Gbps*32 ports. Due to limitations on programmability, we cannot implement Mode-I/III in Tofino. We integrate EPIC with Pytorch, where the CommLib needs to pipeline the memory copy between GPU and RDMA registered buffer and EPIC’s packet I/O. (2) Emulation runs on VMs connected by OVS [59], where host VMs run SoftRoCE, and Mode-I and Mode-II/III switch VMs have IncEngine built atop libibverbs and libcap. (3) Simulations are based on NS3 or OMNET++, which run on a PC.

Topology. We use the following notion to describe the topology “Tree- x - y ”, where x means tree depth and y means tree branches at non-leaf nodes. For example, a star topology with four servers is denoted as Tree-2-4 (servers counted as one tier, and the switch as another).

Workloads. We run two kinds of workloads: (1) Collective communication of the 6 primitives to study communication acceleration, (2) single training job to study EPIC’s acceleration, and (3) multi-tenant training to study resource management. In multi-tenant training, we use job traces from production clusters [6].

Baselines. In testbed experiments, we compare EPIC with NCCL (Ring and Tree); for AllReduce specifically, we compare EPIC with ATP and SwitchML⁶. In packet/flow-level simulation, we compare EPIC with ring-based algorithm. In emulation, we compare EPIC with MPI (uses CPU memory instead of GPU; more suitable for VMs). In the experiment description, we use EPIC-I/II/III to denote EPIC’s three modes.

Metrics. We measure the following metrics to compare solutions: (1) collective’s algorithm throughput, which is the application data size of the ranks divided by the overall collective completion time, and (2) job completion time (JCT).

7.2 Feasibility

Correctness. We run model checking with the Tree-3-2 topology, and verify Mode-II/III’s AllReduce, Reduce, and Broadcast. The network environment is set reliable, lossy, and out-of-order. In all environments, EPIC is correct: the computation result is equivalent to a single server’s result, and the protocol eventually terminates.

Interoperability. Table 3 shows AllReduce throughput in emulation. All three modes in EPIC interoperate with host-side SoftRoCE correctly. And they all give correct results and

⁶We compare with SwitchML DPDK version. SwitchML provides an RDMA UC version, where the RDMA is configured without reliability guarantee, and the host still needs to spare CPU to handle transmission failures.

Table 3: [Emulation, Tree-3-2] AllReduce Algorithm Throughput (Gbps)

Msg. Size (B)	4K	16K	64K	256K	1M	4M	16M	64M	256M	1G
EPIC-I	2.47	10.24	35.9	79.0	182	248	382	418	426	427
EPIC-II	14.7	48.1	67.3	85.1	89.0	93.7	86.6	89.3	94.1	97.9
EPIC-III	15.7	64.1	88.7	86.8	72.5	75.5	74.9	75.5	75.1	75.6
MPI	1.71	3.72	14.9	21.1	73.9	181	316	249	434	502

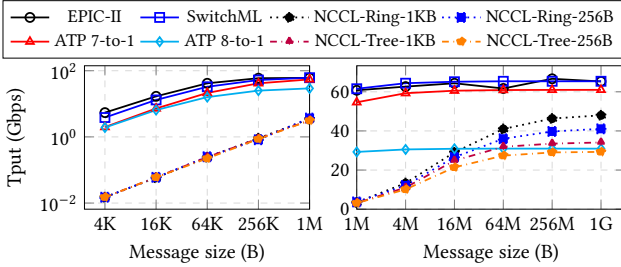


Figure 12: [Testbed, Tree-2-8] AllReduce Algorithm Throughput

finish normally. EPIC-III has more complex switch workflow, so its throughput is lower than EPIC-II. It is hard to make a fair performance comparison (and not the goal of emulation) among EPIC-I vs EPIC-II/III vs MPI, because their software stack differs (details in Appendix §J).

Evolvability. The development of EPIC-II and III follows the modular design. EPIC-II and III consist of 7604 and 7400 lines of code, respectively, with 61% reuse. Switch vendors can iterate INC feature from EPIC-II to EPIC-III, with correctness guarantee while keeping improving performance.

Resource Affordability. Across various hardware, EPIC requires only 1–16 MB of on-chip SRAM, with platforms such as Intel Tofino, Agilex 7 FPGA, and Xilinx VU13P supporting 8 MB, 16 MB, and 1 MB, respectively (§M, §I). For Mode-II, the most memory-intensive realization, a 100 Gbps network with 10 μ s RTT necessitates only 250 KB per job (twice the path BDP). Simulations confirm that even a 1 MB allocation—supporting four concurrent groups—significantly boosts performance in 3D training and multi-tenant environments, thereby reducing JCT despite memory constraints (§L). So the resource cost of EPIC is affordable in production scenarios.

Chip Area. Evaluated by a chip vendor, when synthesized using a 28 nm process technology, EPIC’s IncEngine instance, configured with 512 FP32 ALUs, 512 UINT ALUs and a 1 MB payload buffer, occupies an area of 4.89 mm². The total area overhead for the eight integrated engines (25.6 Tbps) amounts to 39.12 mm², demonstrating a scalable and efficient footprint for high-bandwidth INC.

7.3 Performance Acceleration from INC

Collective Communication. Figure 12 shows AllReduce performance on testbed. All INC solutions consistently outperform the baseline NCCL. For small messages, INC pro-

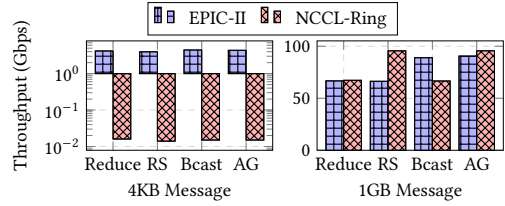


Figure 13: [Testbed, Tree-2-8] Collective Algorithm Throughput

vides a significant lower end-to-end latency due to reduced hop counts and a thinner software stack. For large messages, the performance gain stems from the substantial reduction in network traffic volume.

When the link capacity is saturated for all solutions, INC solutions—EPIC, ATP, and SwitchML—outperforms NCCL. But EPIC spends less CPU resources to saturate links due to its RoCE-compatibility and hardware transmission offloading. SwitchML achieves high throughput using a DPDK-based end-host implementation; however, because DPDK lacks transport-layer reliability, SwitchML must handle packetization and retransmissions, leading to higher CPU overhead compared to EPIC (1 core vs. 6 cores). While ATP performs well with a dedicated Parameter Server (PS) on additional links, its small-message latency remains high, and throughput drops when the PS competes for bandwidth with workers (ATP 8-to-1).

Tofino constrains EPIC’s packet payload size as 256B. Comparing NCCL with 256B payloads, EPIC achieves a 1.59 \times speedup. NCCL with 1KB payloads improves efficiency, which suggests that future EPIC support for larger payloads would yield greater gains. Finally, the NCCL Tree algorithm suffers from the overhead of multiple binomial rounds, proving less effective than the pipelined Ring approach. When performing Barrier, EPIC takes \sim 5 μ s for one operation, while NCCL takes \sim 2 ms. EPIC outperforms NCCL by 400 \times .

Figure 13 shows results across four primitives. EPIC provides a significant advantage for small messages, due to reduced hop counts and minimal software overhead. For large-scale data transfers, NCCL’s Reduce/Broadcast shows a similar throughput due to their ring-based algorithm; EPIC outperforms NCCL in Broadcast due to less traffic to switch, but equals NCCL in Reduce due to the computation overhead in switch. In terms of ReduceScatter and AllGather, NCCL performs concurrent rings so its throughput surges, EPIC keeps RS/AG similar to Reduce/Broadcast because its sequential execution, but EPIC causes less traffic to the network.

Traffic Volume Reduction. We evaluate overlapping ReduceScatter (RS) and AllGather (AG) operations across two communication groups in NCCL and EPIC. The result is shown in Figure 14. In NCCL, aggregate throughput is capped by line rate because nodes must simultaneously transmit and

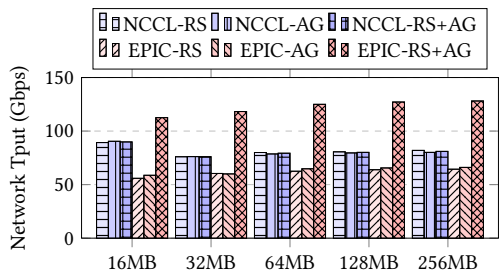


Figure 14: [Testbed, Tree-2-8] Bandwidth Completions between ReduceScatter and AllGather

receive for both ring-based collectives, causing bandwidth contention. Conversely, EPIC breaks this limit by exploiting directional link independence. By orchestrating nodes to transmit for RS while receiving for AG (and vice versa), EPIC ensures non-overlapping directional flows. Consequently, EPIC achieves a theoretical throughput of $2\times$ the link bandwidth, as evidenced by the additive throughput observed in our experiments.

Training Applications. We train three models (GPT-2 Large, Qwen2.5, Llama-3.2) and report their iteration times in Table 4. EPIC accelerates DP and TP by 1.4% and 31.1% (Llama-3.2). Meanwhile, packet-level simulation based on SimAI [74] and NS3 reports a 1.3%–34.7% speedups for Llama-7B to GPT-3-175B (Appendix §K).

This experiment assesses EPIC’s acceleration across various parallel strategies rather than comparing the inherent efficiency of DP versus TP. While EPIC improves both, the speedup is more pronounced in TP due to its higher communication intensity, whereas DP yields more modest gains from its relatively lower volume. Considering cluster architecture, EPIC excels when TP is deployed on scaleouts, but it does not when TP and INC are deployed on “high-bandwidth” scaleups, because the TP AllReduce time is reduced due to high bandwidth, which also reduces INC’s improvement space (Table 6’s last column is improved by 0-0.79% when applying INC on scaleups).

Note that this experiment does not aim to discover whether the experimented models favor DP or TP in training, but rather to show the acceleration to TP/DP. In large-scale training where model shards exceed single-GPU memory, TP is indispensable. For environments utilizing consumer-grade GPUs lacking high-end interconnects (e.g., NVLink), TP traffic frequently becomes the primary bottleneck. In these common scenarios—including fine-tuning and post-training—EPIC delivers significant performance dividends.

Inference Applications. We infer GPT-2 small/large with TP=4 and sequence length=1024 (Table 5). EPIC reduces GPT-2 large’s TTFT/TPOT by 29.1%/30.8%, respectively. For inference’s small-message patterns, EPIC’s reduced hops and latency translate directly into end-to-end performance gains.

Table 4: [Testbed, Tree-2-8] Model Training Iteration Time (s), context_length=2K, batch_size=256.

	Model	EPIC-II	SwitchML	ATP	NCCL
DP=8	GPT-2 Large	5.46	5.48	5.51	5.53
	Qwen2.5-0.5B	3.59	3.61	3.62	3.64
	Llama-3.2-1B	7.18	7.22	7.24	7.28
TP=8	GPT-2 Large	21.79	24.33	26.62	29.35
	Qwen2.5-0.5B	13.10	14.58	15.92	17.51
	Llama-3.2-1B	21.63	23.88	25.93	28.35

Table 5: [Testbed, Tree-2-4] Inference Performance

Performance (ms)	GPT-2 Small		GPT-2 Large	
	TTFT	TPOT	TTFT	TPOT
EPIC-II	12.03	8.809	26.83	25.09
NCCL	13.03	10.05	37.85	36.27

7.4 Loss Tolerance

To study loss tolerance, simulations were conducted using an idealized model where congestion control is disabled, forcing the sender to saturate link bandwidth while prioritizing retransmissions for lost packets.

Throughput vs Loss Rate. This setup allows for a rigorous comparison of EPIC-II and EPIC-III by tuning the packet loss rate on a single link. While both modes see throughput decline as loss rates rise, EPIC-II experiences a sharp collapse after a 10% loss rate. This occurs because a single lost packet in EPIC-II triggers redundant retransmissions across all ranks for that sequence number, whereas EPIC-III allows lossless ranks to receive ACKs and continue, preventing excessive retransmission.

Throughput vs Lossy Links. Further experiments maintaining a constant 5% loss rate while increasing the number of lossy links reveal that EPIC-II suffers more severe degradation than EPIC-III. In EPIC-II, the throughput decline is the cumulative result of losses across all affected links, creating a stacked decrease effect. Conversely, in EPIC-III, the overall performance is determined only by the link with the highest loss rate, as the retransmission times on other links are effectively masked by the most bottlenecked one.

Rate Synchronization for EPIC-III. We run AllReduce on Tree-2-8 with 200 Gbps link capacity. One link is congested by background traffic to 100 Gbps. We apply DCQCN on ranks. Full results are in Table 35 of Appendix §K. Without rate synchronization (switch replying CNP to faster ranks),

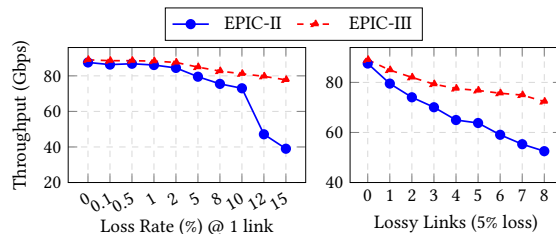


Figure 15: [Packet Simulation, Tree-2-8] AllReduce Algorithm Throughput

Table 6: [Flow Simulation] JCT (three iterations) of GPT3-175B on 128-GPU Fat-tree

SRAM (Unit)	w/o scaleup		w/ scaleup	
	4	8	4	8
Ring	253	253	106	106
EDT	179	179	84.6	84.6
Spatial Mux	179	158	84.6	63.6
Temporal Mux	158	137	84.6	63.6

the algorithm throughput is 43.3 Gbps (16 MB message); with rate synchronization, the throughput becomes 95.9 Gbps. Applying congestion control-based rate synchronization can avoid excessive sending and dropping, thereby improving the overall collective throughput.

7.5 Performance Gain from Policy

Single 3D Parallel Training Job. Table 6 shows a single training job. We tune switch SRAM sizes based on BDP-relative units (§5). Groups select candidate aggregation trees greedily following our algorithms (§6.2). Ring-based NCCL serves as the baseline, yielding the longest JCT due to lack of INC acceleration. The EDT policy suffers from placement conflicts, leaving several communication groups without INC resources.

In contrast, Spatial Mux grants more groups INC access when resources permit. Temporal Mux further maximizes benefits by sharing limited resources across groups, benefiting the entire workload (up to 1.85×). Integrating scaleup networks yields similar conclusions, though overall INC acceleration gains diminish as high-bandwidth scaleup links absorb significant traffic, reducing relative network transmission time (1.67×).

Multi-tenant Training Jobs. Figure 16 shows the simulation results of multi-tenant training on a 2,048-GPU cluster with production trace [6], varying INC management policies. Compared to the baseline, all INC-enabled policies significantly reduce the average Job Completion Time (JCT). Among these strategies, Temporal Mux achieves the highest overall acceleration.

JCT distribution analysis reveals that while Temporal Mux is less efficient than EDT for jobs in the 88th to 98th percentiles, it drastically reduces tail latency. At the 99th percentile, JCTs for Temporal Mux, EDT, and Ring are 4917 s, 5420 s, and 7115 s, respectively. This improvement stems from Temporal Mux allowing all jobs to contend for INC resources; previously blocked jobs gain acceleration, while formerly exclusive jobs face only minor interference.

8 RELATED WORK

INC Primitive Design. Many existing programmable switch-based INC solutions focus on certain primitives (e.g., AllReduce [8, 19, 36, 40, 44–46, 50, 64, 78], Broadcast [28, 34, 43]), which belong to EPIC Mode-II; EPIC supports six primitives

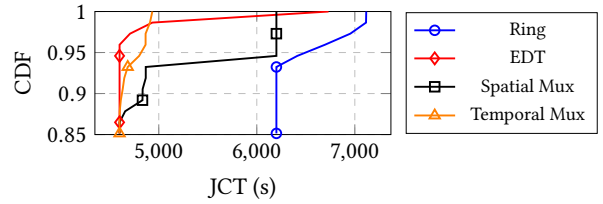


Figure 16: [Flow Simulation] Tail 15% JCT of Alibaba Trace on 2048-GPU Fat-tree

and hybrid invocations through specialized control signals and group PSN synchronization, and fixes their bugs by model checking. There are product switches with six collectives supported [5, 20, 21], which belong to EPIC Mode-I; EPIC proposes a modular design and supports evolvability from simple to complex. The Ultra Ethernet Consortium is finalizing the INC standard [70], which is a clean-slate, Mode-I-like design with an INC header and UET transport. There are in-network computing solutions for irregular traffic patterns [22, 29] and generic computing [71, 77, 80], which we would consider in the future.

INC Resource Management. INC management in a cluster should consider function placement [3, 66], routing [12, 14, 63, 65, 76, 83], job placement [81], and resource allocation [79]; EPIC provides a unified resource model to enable these policies.

INC Switch Micro Architecture. EPIC focus on protocol design, and is compatible with existing switch micro architecture designs [7, 72].

Modular Network Design. There were modular design of software switch/router [9, 37, 58], network functions [16, 52], and network layers [13]. EPIC differs from them in the application scenario: it implements the same functionality with different algorithms and applies modularity to enable algorithm evolution. ClickINC [77] implements the same algorithms on different platforms. Click [37] uses modules to flexibly compose different functionalities. P4 [4] provides a platform-independent language to program different functionalities.

Collective Communication Libraries. There are various collective communication libraries and their optimizations [1, 11, 23, 32, 35, 53, 54, 67]; EPIC’s CommLib works at the same layer and should be integrated within mainstream CCLs.

9 CONCLUSION

To address Ethernet fragmentation in INC, we propose EPIC protocol featuring unified abstraction and polymorphic realization. Its modular design allows seamless, incremental hardware evolution while maintaining protocol integrity. Validated via model checking, EPIC ensures robust performance across diverse conditions. EPIC unifies resource management and enhances control-plane agility. EPIC signifi-

cantly accelerates collective communication, and reduces single- and multi-tenant training JCT.

REFERENCES

- [1] AMD. 2024. RCCL. (2024). <https://github.com/ROCm/rccl>.
- [2] Wei Bai, Shanin Sainul Abdeen, Ankit Agrawal, Krishan Kumar Attre, Paramvir Bahl, Ameya Bhagat, Gowri Bhaskara, Tanya Brokhman, Lei Cao, Ahmad Cheema, et al. 2023. Empowering azure storage with RDMA. In *20th USENIX Symposium on Networked Systems Design and Implementation (NSDI 23)*. 49–67.
- [3] Marcel Blöcher, Lin Wang, Patrick Eugster, and Max Schmidt. 2021. Switches for HIRE: Resource scheduling for data center in-network computing. In *Proceedings of the 26th ACM International Conference on Architectural Support for Programming Languages and Operating Systems*. 268–285.
- [4] Pat Bosshart, Dan Daly, Glen Gibb, Martin Izzard, Nick McKeown, Jennifer Rexford, Cole Schlesinger, Dan Talayco, Amin Vahdat, George Varghese, et al. 2014. P4: Programming protocol-independent packet processors. *ACM SIGCOMM Computer Communication Review* 44, 3 (2014), 87–95.
- [5] Broadcom Inc. 2026. StrataXGS Tomahawk 5 Series: 51.2 Tb/s Ethernet Switch ASIC Family. <https://www.broadcom.com/products/ethernet-connectivity/switching/strataxgs/bcm78920-series>. (2026). Accessed: 2026-02-06.
- [6] Jiamin Cao, Yu Guan, Kun Qian, Jiaqi Gao, Wencong Xiao, Jianbo Dong, Binzhang Fu, Dennis Cai, and Ennan Zhai. 2024. Crux: Gpu-efficient communication scheduling for deep learning training. In *Proceedings of the ACM SIGCOMM 2024 Conference*. 1–15.
- [7] Daniele De Sensi, Salvatore Di Girolamo, Saleh Ashkboos, Shigang Li, and Torsten Hoefler. 2021. Flare: Flexible in-network allreduce. In *Proceedings of the International Conference for High Performance Computing, Networking, Storage and Analysis*. 1–16.
- [8] Salvatore Di Girolamo, Andreas Kurth, Alexandru Calotoiu, Thomas Benz, Timo Schneider, Jakub Beránek, Luca Benini, and Torsten Hoefler. 2021. A RISC-V in-network accelerator for flexible high-performance low-power packet processing. In *2021 ACM/IEEE 48th Annual International Symposium on Computer Architecture (ISCA)*. IEEE, 958–971.
- [9] Mihai Dobrescu, Norbert Egi, Katerina Argyraki, Byung-Gon Chun, Kevin Fall, Gianluca Iannaccone, Allan Knies, Maziar Manesh, and Sylvia Ratnasamy. 2009. RouteBricks: Exploiting parallelism to scale software routers. In *Proceedings of the ACM SIGOPS 22nd symposium on Operating systems principles*. 15–28.
- [10] Jianbo Dong, Bin Luo, Jun Zhang, Pengcheng Zhang, Fei Feng, Yikai Zhu, Ang Liu, Zian Chen, Yi Shi, Hairong Jiao, et al. 2024. Boosting large-scale parallel training efficiency with c4: A communication-driven approach. *arXiv preprint arXiv:2406.04594* (2024).
- [11] Jianbo Dong, Shaochuang Wang, Fei Feng, Zheng Cao, Heng Pan, Lingbo Tang, Pengcheng Li, Hao Li, Qianyuan Ran, Yiqun Guo, et al. 2021. ACCL: Architecting Highly Scalable Distributed Training Systems with Highly Efficient Collective Communication Library. *IEEE Micro* 41, 5 (2021), 85–92.
- [12] Shichen Dong, Zhixiong Niu, Mingchao Zhang, Zhiying Xu, Chuntao Hu, Pengzhi Zhu, Qingchun Song, Lei Qu, Peng Cheng, Cam-Tu Nguyen, et al. 2025. Mina: Fine-Grained In-network Aggregation Resource Scheduling for Machine Learning Service. In *IEEE INFOCOM 2025-IEEE Conference on Computer Communications*. IEEE, 1–10.
- [13] Cheng Tien Ee, Rodrigo Fonseca, Sukun Kim, Daekyeong Moon, Arsalan Tavakoli, David E Culler, Scott Shenker, and Ion Stoica. 2006. A Modular Network Layer for Sensornets.. In *OSDI*, Vol. 6. 249–262.
- [14] Jin Fang, Gongming Zhao, Hongli Xu, Changbo Wu, and Zhuolong Yu. 2023. GRID: Gradient routing with in-network aggregation for distributed training. *IEEE/ACM Transactions on Networking* 31, 5 (2023), 2267–2280.
- [15] Edgar Gabriel, Graham E. Fagg, George Bosilca, Thara Angskun, Jack J. Dongarra, Jeffrey M. Squyres, Vishal Sahay, Prabhanjan Kambadur, Brian Barrett, Andrew Lumsdaine, Ralph H. Castain, David J. Daniel, Richard L. Graham, and Timothy S. Woodall. 2004. Open MPI: Goals, Concept, and Design of a Next Generation MPI Implementation. In *Proceedings of the 11th European PVM/MPI Users' Group Meeting*. Budapest, Hungary.
- [16] Massimo Gallo and Rafael Laufer. 2018. ClickNF: a Modular Stack for Custom Network Functions. In *2018 USENIX Annual Technical Conference (USENIX ATC 18)*. 745–757.
- [17] Adithya Gangidi, Rui Miao, Shengbao Zheng, Sai Jayesh Bondu, Guilherme Goes, Hany Morsy, Rohit Puri, Mohammad Riftadi, Ashmitha Jeevaraj Shetty, Jingyi Yang, et al. 2024. Rdma over ethernet for distributed training at meta scale. In *Proceedings of the ACM SIGCOMM 2024 Conference*. 57–70.
- [18] Yixiao Gao, Qiang Li, Lingbo Tang, Yongqing Xi, Pengcheng Zhang, Wenwen Peng, Bo Li, Yaohui Wu, Shaozong Liu, Lei Yan, et al. 2021. When cloud storage meets RDMA. In *18th USENIX Symposium on Networked Systems Design and Implementation (NSDI 21)*. 519–533.
- [19] Nadeen Gebara, Manya Ghobadi, and Paolo Costa. 2021. In-network aggregation for shared machine learning clusters. *Proceedings of Machine Learning and Systems* 3 (2021), 829–844.
- [20] Richard L Graham, Devendar Bureddy, Pak Lui, Hal Rosenstock, Gilad Shainer, Gil Bloch, Dror Goldener, Mike Dubman, Sasha Kotchubievsky, Vladimir Koushnr, et al. 2016. Scalable hierarchical aggregation protocol (SHARp): A hardware architecture for efficient data reduction. In *2016 First International Workshop on Communication Optimizations in HPC (COMHPC)*. IEEE, 1–10.
- [21] Richard L Graham, Lion Levi, Devendar Burreddy, Gil Bloch, Gilad Shainer, David Cho, George Elias, Daniel Klein, Joshua Ladd, Ophir Maor, et al. 2020. Scalable hierarchical aggregation and reduction protocol (sharp) tm streaming-aggregation hardware design and evaluation. In *International Conference on High Performance Computing*. Springer, 41–59.
- [22] Yongchao He, Wenfei Wu, Yanfang Le, Ming Liu, and ChonLam Lao. 2023. A generic service to provide in-network aggregation for key-value streams. In *Proceedings of the 28th ACM International Conference on Architectural Support for Programming Languages and Operating Systems, Volume 2*. 33–47.
- [23] Mert Hidayetoglu, Simon Garcia de Gonzalo, Elliott Slaughter, Pinku Surana, Wen-mei Hwu, William Gropp, and Alex Aiken. 2024. HiCCL: A Hierarchical Collective Communication Library. *arXiv preprint arXiv:2408.05962* (2024).
- [24] Torsten Hoefler, Tommaso Bonato, Daniele De Sensi, Salvatore Di Girolamo, Shigang Li, Marco Heddes, Deepak Goel, Miguel Castro, and Steve Scott. 2024. Hammingmesh: A network topology for large-scale deep learning. *Commun. ACM* 67, 12 (2024), 97–105.
- [25] Torsten Hoefler, Mikhail Khalilov, Josiah Clark, Surendra Anubolu, Mohan Kalkunte, Karen Schramm, Eric Spada, Duncan Roweth, Keith Underwood, Adrian Caulfield, et al. 2025. In-Network Collective Operations: Game Changer or Challenge for AI Workloads? *Computer* 59, 1 (2025), 24–33.
- [26] Torsten Hoefler, Andrew Lumsdaine, and Wolfgang Rehm. 2007. Implementation and performance analysis of non-blocking collective operations for MPI. In *Proceedings of the 2007 ACM/IEEE conference on Supercomputing*. 1–10.
- [27] Torsten Hoefler and Dmitry Moor. 2014. Energy, memory, and runtime tradeoffs for implementing collective communication operations. *Supercomputing frontiers and innovations* 1, 2 (2014), 58–75.
- [28] Chengyuan Huang, Yixiao Gao, Wei Chen, Duoxing Li, Yibo Xiao, Ruyi Zhang, Chen Tian, Xiaoliang Wang, Wanchun Dou, Guihai Chen, et al. 2023. MC-RDMA: Improving Replication Performance of RDMA-based Distributed Systems with Reliable Multicast Support. In *2023 IEEE 31st*

- International Conference on Network Protocols (ICNP)*. IEEE, 1–11.
- [29] Guyue Huang, Hao Li, Le Qin, Jiayi Huang, Yangwook Kang, Yufei Ding, and Yuan Xie. 2025. TRACI: Network Acceleration of Input-Dynamic Communication for Large-Scale Deep Learning Recommendation Model. In *Proceedings of the 52nd Annual International Symposium on Computer Architecture*. 1880–1893.
- [30] InfiniBand Trade Association. [n. d.]. *Supplement to InfiniBand™ Architecture Specification Volume 1 Release 1.2.1: Annex A17: RoCEv2*. Technical Specification Supplement Release 1.2.1, Annex A17. InfiniBand Trade Association. Proprietary document; available via InfiniBand Trade Association membership.
- [31] Intel. 2024. Intel Tofino 2. (2024). <https://www.intel.com/content/www/us/en/products/details/network-io/intelligent-fabric-processors/tofino-2.html>
- [32] Intel. 2024. oneAPI Collective Communications Library (oneCCL). (2024). <https://github.com/oneapi-src/oneCCL>.
- [33] Norm Jouppi, George Kurian, Sheng Li, Peter Ma, Rahul Nagarajan, Lifeng Nai, Nishant Patil, Suvinay Subramanian, Andy Swing, Brian Towles, et al. 2023. Tpu v4: An optically reconfigurable supercomputer for machine learning with hardware support for embeddings. In *Proceedings of the 50th annual international symposium on computer architecture*. 1–14.
- [34] Mikhail Khalilov, Salvatore Di Girolamo, Marcin Chrapek, Rami Nudelman, Gil Bloch, and Torsten Hoefler. 2024. Network-offloaded bandwidth-optimal broadcast and Allgather for distributed AI. In *SC24: International Conference for High Performance Computing, Networking, Storage and Analysis*. IEEE, 1–17.
- [35] Heehoon Kim, Junyeol Ryu, and Jaejin Lee. 2024. TCCL: Discovering Better Communication Paths for PCIe GPU Clusters. In *Proceedings of the 29th ACM International Conference on Architectural Support for Programming Languages and Operating Systems, Volume 3*. 999–1015.
- [36] Benjamin Klenk, Nan Jiang, Greg Thorson, and Larry Dennison. 2020. An in-network architecture for accelerating shared-memory multi-processor collectives. In *2020 ACM/IEEE 47th Annual International Symposium on Computer Architecture (ISCA)*. IEEE, 996–1009.
- [37] Eddie Kohler, Robert Morris, Benjie Chen, John Jannotti, and M Frans Kaashoek. 2000. The Click modular router. *ACM Transactions on Computer Systems (TOCS)* 18, 3 (2000), 263–297.
- [38] Leslie Lamport. 2002. *Specifying systems: The TLA+ language and tools for hardware and software engineers*. Addison-Wesley.
- [39] ChonLam Lao, Jiaqi Gao, Jiamin Cao, Zhipeng Zhang, Pengcheng Zhang, Jiangfei Duan, Minlan Yu, Aditya Akella, Zhilong Zheng, Yu Guan, Yichi Xu, Yong Li, Ennan Zhai, Dennis Cai, Zhengping Qian, and Jingren Zhou. 2026. Continuum: An Interruption-Resilient Runtime for ML Training. In *OSDI*.
- [40] ChonLam Lao, Yanfang Le, Kshiteej Mahajan, Yixi Chen, Wenfei Wu, Aditya Akella, and Michael Swift. 2021. ATP: In-network aggregation for multi-tenant learning. In *18th USENIX Symposium on Networked Systems Design and Implementation (NSDI 21)*. 741–761.
- [41] Wenxue Li, Xiangzhou Liu, Yuxuan Li, Yilun Jin, Han Tian, Zhizhen Zhong, Guyue Liu, Ying Zhang, and Kai Chen. 2024. Understanding communication characteristics of distributed training. In *Proceedings of the 8th Asia-Pacific Workshop on Networking*. 1–8.
- [42] Wenxue Li, Xiangzhou Liu, Yunxuan Zhang, Zihao Wang, Wei Gu, Tao Qian, Gaoxiong Zeng, Shoushou Ren, Xinyang Huang, Zhenghang Ren, et al. 2025. Revisiting RDMA Reliability for Lossy Fabrics. In *Proceedings of the ACM SIGCOMM 2025 Conference*. 85–98.
- [43] Wenxue Li, Junyi Zhang, Yufei Liu, Gaoxiong Zeng, Zilong Wang, Chaoliang Zeng, Pengpeng Zhou, Qiaoling Wang, and Kai Chen. 2024. Cepheus: accelerating datacenter applications with high-performance roce-capable multicast. In *2024 IEEE International Symposium on High-Performance Computer Architecture (HPCA)*. IEEE, 908–921.
- [44] Youjie Li, Iou-Jen Liu, Yifan Yuan, Deming Chen, Alexander Schwing, and Jian Huang. 2019. Accelerating distributed reinforcement learning with in-switch computing. In *Proceedings of the 46th International Symposium on Computer Architecture*. 279–291.
- [45] Zhaoyi Li, Jiawei Huang, Yijun Li, Aikun Xu, Shengwen Zhou, Jingling Liu, and Jianxin Wang. 2023. A2TP: Aggregator-aware in-network aggregation for multi-tenant learning. In *Proceedings of the Eighteenth European Conference on Computer Systems*. 639–653.
- [46] Zhaoyi Li, Jiawei Huang, Tao Zhang, Shengwen Zhou, Qile Wang, Yijun Li, Jingling Liu, Wanchun Jiang, and Jianxin Wang. 2023. PA-ATP: Progress-Aware Transmission Protocol for In-Network Aggregation. In *2023 IEEE 31st International Conference on Network Protocols (ICNP)*. IEEE, 1–11.
- [47] Linux man-pages project. [n. d.]. rxe(7): Software RDMA over Ethernet (RoCE) driver. ([n. d.]). <https://man7.org/linux/man-pages/man7/rxe.7.html> Documents Linux kernel module rdma_rxe (Soft-RoCE/RXE).
- [48] Linux RDMA Community. 2024. libibverbs: Userspace InfiniBand Verbs Library. <https://github.com/linux-rdma/rdma-core/tree/master/libibverbs>. (2024). Part of rdma-core; provides the ibv_* API for RDMA device management, QP/CQ/MR operations, and data transfer.
- [49] Aixin Liu, Bei Feng, Bing Xue, Bingxuan Wang, Bochao Wu, Chengda Lu, Chenggang Zhao, Chengqi Deng, Chenyu Zhang, Chong Ruan, et al. 2024. Deepseek-v3 technical report. *arXiv preprint arXiv:2412.19437* (2024).
- [50] Shuo Liu, Qiaoling Wang, Junyi Zhang, Wenfei Wu, Qinliang Lin, Yao Liu, Meng Xu, Marco Canini, Ray CC Cheung, and Jianfei He. 2023. In-network aggregation with transport transparency for distributed training. In *Proceedings of the 28th ACM International Conference on Architectural Support for Programming Languages and Operating Systems, Volume 3*. 376–391.
- [51] Qingkai Meng, Hao Zheng, Zhenhui Zhang, ChonLam Lao, Chengyuan Huang, Baojia Li, Ziyuan Zhu, Hao Lu, Weizhen Dang, Zitong Lin, et al. 2025. Astral: A datacenter infrastructure for large language model training at scale. In *Proceedings of the ACM SIGCOMM 2025 Conference*. 609–625.
- [52] Zili Meng, Jun Bi, Haiping Wang, Chen Sun, and Hongxin Hu. 2019. MicroNF: An efficient framework for enabling modularized service chains in NFV. *IEEE Journal on Selected Areas in Communications* 37, 8 (2019), 1851–1865.
- [53] Microsoft. 2023. MSCCL. (2023). <https://github.com/microsoft/msccl>.
- [54] NVIDIA. 2024. NCCL. (2024). <https://github.com/NVIDIA/nccl>.
- [55] NVIDIA Corporation. [n. d.]. *NVIDIA NVLink High-Speed Interconnect: Application Performance*. Whitepaper. NVIDIA Corporation.
- [56] OMNeT++ Community. 2024. OMNeT++ Discrete Event Simulator. <https://omnetpp.org>. (2024). Version 6.2.
- [57] OpenInfra Foundation. [n. d.]. OpenStack: Open source cloud computing infrastructure. ([n. d.]). <https://www.openstack.org/>
- [58] Aurojit Panda, Sangjin Han, Keon Jang, Melvin Walls, Sylvia Ratnasamy, and Scott Shenker. 2016. NetBricks: Taking the V out of NFV. In *12th USENIX Symposium on Operating Systems Design and Implementation (OSDI 16)*. 203–216.
- [59] Ben Pfaff, Justin Pettit, Teemu Koponen, Ethan J. Jackson, Andy Zhou, Jarno Rajahalme, Jesse Gross, Alex Wang, Jonathan Stringer, Pravin Shelar, Keith Amidon, and Martin Casado. 2015. The Design and Implementation of Open vSwitch. In *12th USENIX Symposium on Networked Systems Design and Implementation (NSDI '15)*. USENIX Association, 117–130. <https://www.usenix.org/system/files/conference/nsdi15/nsdi15-paper-pfaff.pdf>
- [60] Chenchen Qi, Wenfei Wu, Yongcan Wang, Keqiang He, Yu-Hsiang Kao, Zongying He, Chen-Yu Yen, Zhuo Jiang, Feng Luo, Surendra Anubolu, et al. 2025. SGLB: Scalable and Robust Global Load Balancing in Commodity AI Clusters. In *Proceedings of the ACM SIGCOMM 2025*

- Conference*. 626–644.
- [61] Kun Qian, Yongqing Xi, Jiamin Cao, Jiaqi Gao, Yichi Xu, Yu Guan, Binzhang Fu, Xuemei Shi, Fangbo Zhu, Rui Miao, et al. 2024. Alibaba hpn: A data center network for large language model training. In *Proceedings of the ACM SIGCOMM 2024 Conference*. 691–706.
- [62] Samyam Rajbhandari, Jeff Rasley, Olatunji Ruwase, and Yuxiong He. 2020. Zero: Memory optimizations toward training trillion parameter models. In *SC20: International Conference for High Performance Computing, Networking, Storage and Analysis*. IEEE, 1–16.
- [63] Ori Rottenstreich and Jose Yallouz. 2024. Edge-disjoint tree allocation for multi-tenant cloud security in datacenter topologies. *IEEE/ACM Transactions on Networking* 32, 4 (2024), 2858–2874.
- [64] Amedeo Sapio, Marco Canini, Chen-Yu Ho, Jacob Nelson, Panos Kalnis, Changhoon Kim, Arvind Krishnamurthy, Masoud Moshref, Dan Ports, and Peter Richtárik. 2021. Scaling distributed machine learning with In-Network aggregation. In *18th USENIX Symposium on Networked Systems Design and Implementation (NSDI 21)*. 785–808.
- [65] Raz Segal, Chen Avin, and Gabriel Scalosub. 2021. SOAR: Minimizing network utilization with bounded in-network computing. In *Proceedings of the 17th International Conference on emerging Networking EXperiments and Technologies*. 16–29.
- [66] Raz Segal, Chen Avin, and Gabriel Scalosub. 2022. Constrained in-network computing with low congestion in datacenter networks. In *IEEE INFOCOM 2022-IEEE Conference on Computer Communications*. IEEE, 1639–1648.
- [67] Aashaka Shah, Vijay Chidambaram, Meghan Cowan, Saeed Maleki, Madan Musuvathi, Todd Mytkowicz, Jacob Nelson, Olli Saarikivi, and Rachee Singh. 2023. TACCL: Guiding Collective Algorithm Synthesis using Communication Sketches. In *20th USENIX Symposium on Networked Systems Design and Implementation (NSDI 23)*. 593–612.
- [68] The Tcpdump Group. [n. d.]. libpcap: Portable packet capture library. ([n. d.]). <https://www.tcpdump.org/>
- [69] UAlink Consortium. 2024. UAlink Consortium. Online Consortium Website. (2024). <https://ualinkconsortium.org/>
- [70] Ultra Ethernet Consortium. 2024. Ultra Ethernet Specification Update. Ultra Ethernet Consortium Blog. (29 August 2024). <https://ultraethernet.org/ultra-ethernet-specification-update/> Accessed: 2026-02-06.
- [71] Xinchun Wan, Luyang Li, Han Tian, Xudong Liao, Xinyang Huang, Chaoliang Zeng, Zilong Wang, Xinyu Yang, Ke Cheng, Qingsong Ning, et al. 2025. A Generic and Efficient Communication Framework for Message-level In-Network Computing. In *IEEE INFOCOM 2025-IEEE Conference on Computer Communications*. IEEE, 1–10.
- [72] Ruiqi Wang, Dezun Dong, Fei Lei, Junchao Ma, Ke Wu, and Kai Lu. 2023. Roar: A router microarchitecture for in-network allreduce. In *Proceedings of the 37th International Conference on Supercomputing*. 423–436.
- [73] Weiyang Wang, Moein Khazraee, Zhizhen Zhong, Manya Ghobadi, Zhihao Jia, Dheevatsa Mudigere, Ying Zhang, and Anthony Kewitsch. 2023. TopoOpt: Co-optimizing network topology and parallelization strategy for distributed training jobs. In *20th USENIX Symposium on Networked Systems Design and Implementation (NSDI 23)*. 739–767.
- [74] Xizheng Wang, Qingxu Li, Yichi Xu, Gang Lu, Dan Li, Li Chen, Heyang Zhou, Linkang Zheng, Sen Zhang, Yikai Zhu, et al. 2025. SimAI: Unifying Architecture Design and Performance Tuning for Large-Scale Large Language Model Training with Scalability and Precision. In *22nd USENIX Symposium on Networked Systems Design and Implementation (NSDI 25)*. 541–558.
- [75] Yongji Wu, Yechen Xu, Jingrong Chen, Zhaodong Wang, Ying Zhang, Matthew Lentz, and Danyang Zhuo. 2024. McCs: A service-based approach to collective communication for multi-tenant cloud. In *Proceedings of the ACM SIGCOMM 2024 Conference*. 679–690.
- [76] Junxu Xia, Wenfei Wu, Lailong Luo, Geyao Cheng, Deke Guo, and Qifeng Nian. 2024. Accelerating and securing federated learning with stateless in-network aggregation at the edge. In *2024 IEEE 44th International Conference on Distributed Computing Systems (ICDCS)*. IEEE, 692–702.
- [77] Wenquan Xu, Zijian Zhang, Yong Feng, Haoyu Song, Zhikang Chen, Wenfei Wu, Guyue Liu, Yinchao Zhang, Shuxin Liu, Zerui Tian, et al. 2023. Clickinc: In-network computing as a service in heterogeneous programmable data-center networks. In *Proceedings of the ACM SIGCOMM 2023 Conference*. 798–815.
- [78] Mingran Yang, Alex Baban, Valery Kugel, Jeff Libby, Scott Mackie, Swamy Sadashivaiah Renu Kananda, Chang-Hong Wu, and Manya Ghobadi. 2022. Using trio: juniper networks’ programmable chipset for emerging in-network applications. In *Proceedings of the ACM SIGCOMM 2022 Conference*. 633–648.
- [79] Bohan Zhao, Chang Liu, Jianbo Dong, Zheng Cao, Wei Nie, and Wenfei Wu. 2023. Enabling switch memory management for distributed training with in-network aggregation. In *IEEE INFOCOM 2023-IEEE conference on computer communications*. IEEE, 1–10.
- [80] Bohan Zhao, Wenfei Wu, and Wei Xu. 2023. NetRPC: Enabling In-Network computation in remote procedure calls. In *20th USENIX symposium on networked systems design and implementation (NSDI 23)*. 199–217.
- [81] Bohan Zhao, Wei Xu, Shuo Liu, Yang Tian, Qiaoling Wang, and Wenfei Wu. 2024. Training job placement in clusters with statistical in-network aggregation. In *Proceedings of the 29th ACM International Conference on Architectural Support for Programming Languages and Operating Systems, Volume 1*. 420–434.
- [82] Yanli Zhao, Andrew Gu, Rohan Varma, Liang Luo, Chien-Chin Huang, Min Xu, Less Wright, Hamid Shojanazeri, Myle Ott, Sam Shleifer, et al. 2023. Pytorch fsdp: experiences on scaling fully sharded data parallel. *arXiv preprint arXiv:2304.11277* (2023).
- [83] Haowen Zhu, Zehua Guo, and Minghao Ye. 2025. DINA: Toward Determined In-Network Aggregation for Distributed Machine Learning. *IEEE Transactions on Networking* (2025).

A SEMANTICS OF COLLECTIVES

AllReduce: Its semantic is to sum up (or perform other reduction operations on) data vectors from all ranks and distribute the result to all ranks. In EPIC IncTree, data streams from leaves to the root, being aggregated at each intermediate node and sent to the parent until reaching the root. The root streams the final result back, and intermediate nodes multicast the result to their children until it reaches the leaves (Figure 2a).

Reduce: Its semantic is to sum up all ranks' data and deliver the result to one specific rank (the root). EPIC configures all non-receivers to stream data toward the receiver along the aggregation tree. Intermediate nodes aggregate incoming data streams into one and forward it toward the receiver. The receiver obtains the intermediate results and adds its own data to produce the final result (Figure 2b).

Broadcast: Its semantic is to send one rank's data to all other ranks. In EPIC, the sender streams data into the tree, and intermediate nodes replicate the data, forwarding it to all neighbors except the incoming interface, ensuring all ranks eventually receive the data copy (Figure 2c).

Barrier: Its semantic is to synchronize the state among members. It is performed as an AllReduce operation with an empty data payload, leveraging the synchronization property of the reduction tree.

ReduceScatter: Its semantic is to reduce data from all members, split the result, and scatter fragments to members. EPIC performs it as multiple Reduce operations.

AllGather: Its semantic is to gather data from all members, concatenate it, and return the concatenated data to all members. EPIC performs this as multiple Broadcast operations.

B INCENGINE ALGORITHMS

Algorithm 1 shows the IncEngine algorithm for Mode-II, and Algorithm 2 shows that for Mode-III. Algorithm 2 can evolve from Algorithm 1 with changes highlighted.

C IMPACT FROM ROCE'S RELIABILITY

Mode-II is compatible with both versions of RoCE reliability mechanisms. (1) Go-Back-N (GBN): Timeouts and NAKs trigger the sender to retransmit from the first missing PSN. EPIC keeps idempotent when processing retransmissions. An optimization is to maintain an *epsn* (expected PSN) in the switch endpoint state, dropping out-of-order packets immediately. This matches the receiver's logic (which would NAK out-of-order packets anyway) and reduces switch buffer access cost. (2) Selective Retransmission (SR): SACKs describe ranges of out-of-order packets. EPIC switches and receiver buffers can handle out-of-order arrival. The complexity arises in Broadcast ACK aggregation, where merging SACK ranges requires computing the intersection of multiple intervals.

Algorithm 1: Algorithm and control flow of Mode-II

```

1 struct Pipe
2   | payload: Address of MTU array; /* in SRAM, $6 */
3   | degree: Address of Int array; /* in SRAM, $6 */
4 struct EndPoint
5   | // configuration
6   | remote: Endpoint;
7   | ip: IP address; qp: QP Number; port: switch port;
8   | // receive states
9   | arrived: Array of Bit;
10 struct Context
11   | // persistent states
12   | N: Int of array size; eps: Array of EndPoint; pipe: Pipe;
13   | // invocation states
14   | collective: Enum; root: Int; firstPsn: Int; lastPsn: Int;
15 while receive a packet pkt do
16   | (ctx, ep, class, fanin, outs) = LookupTable(pkt);
17   | pkt.idx = pkt.psn%ctx.N;
18   | pkt.idx2 = (pkt.psn+ctx.W)%ctx.N;
19   | if class = UP_DATA then
20     | isDup = CheckDuplicate(pkt, ep);
21     | if not isDup then AggregateData(ctx.pipe, pkt);
22     | if ctx.pipe.degree[pkt.idx] < fanin then continue;
23     | pkt.payload = ctx.pipe.payload[pkt.idx];
24     | RecycleBuffer(ctx.pipe, pkt.idx2, pkt.idx2 + 1);
25   | for (pkt', out) ∈ DuplicateData(pkt, outs) do
26     | pkt' = TranslateHeader(pkt', out);
27     | Forward(pkt', out.port);
28 Function CheckDuplicate(pkt, ep):
29   | v=ep.arrived[pkt.idx]; ep.arrived[pkt.idx]=1;
30   | return v==1;
31 Function AggregateData(pipe, pkt):
32   | pipe.payload[pkt.idx] += pkt.payload;
33   | pipe.degree[pkt.idx] += 1;
34 Function RecycleBuffer(pipe, start, end):
35   | for i ∈ [start, end] do
36     | pipe.payload[i]=pipe.degree[i]=0;

```

Given the low packet loss rate in data centers, and effective congestion control and flow control (e.g., credit-based, or priority-based), these corner cases are infrequent.

Mode-III does not confine the selection of reliability mechanism in Mode-III. Both GBN and SR can work correctly in switch nodes. The module Retransmission need to adapt the corresponding packet sending to the selection.

D OTHER POSSIBLE INCENGINE MODES

There could be other modes, representing a tradeoff between complexity, cost, and performance. For example, in Mode-II AllReduce, the switch node can buffer broadcasted result

Algorithm 2: Algorithm and control flow of Mode-III (changes highlighted)

```

1 struct Pipe
2   payload: Address of MTU array;
3   degree: Address of Int array;
4   fromEps: Array of EndPoint;
5   toEps: Array of EndPoint;
6   psnStart: Int;
7 struct EndPoint
8   // configuration
9   remote: Endpoint;
10  ip: IP address; qp: QP Number; port: switch port;
11  // receive states
12  arrived: Array of Bit;   epsn: Int;   fromPipe: Pipe;
13  // send states
14  resend: Timer;   lastAcked: Int;
15  maxPsnSent: Int;   toPipe: Pipe;
16 struct Context
17  N: Int of array size;   eps: Array of EndPoint;
18  collective: Enum; root: Int; first_psn: Int; last_psn: Int;
19  aggPipe: Pipe;   bcastPipe: Pipe;
20 while receive a packet pkt do
21  (ctx, ep, class, fanin, outs) = LookupTable(pkt, table);
22  pkt.idx = pkt.PSN % ctx.N;
23  if pkt is ACK then
24    ReceiveAck(pkt, ep);
25    pipe = ep.fromPipe; eps = pipe.toEps;
26    psnStart0 = pipe.psnStart;
27    pipe.psnStart = Min([e.lastAcked | e ∈ eps]) + 1;
28    RecycleBuffer(pipe, psnStart0, pipe.psnStart);
29    continue;
30  pipe = ep.toPipe; toSend = 0;
31  if pkt.psn ∉ [pipe.psnStart, pipe.psnStart + N) then
32    continue;
33  isDup ← CheckDuplicate(pkt, ep);
34  while ep.arrived[ep.epsn] == 1 do ep.epsn++;
35  toSend.add(SendAck(pkt, ep));
36  if isDup then goto FORWARD;
37  AggregateData(pkt, pipe);
38  if pipe.degree[pkt.idx] < fanin then goto FORWARD;
39  pkt.payload = pipe.payload[pkt.idx];
40  for out ∈ outs do
41    pkt1 = TranslateHeader(pkt, out);
42    out.maxPsnSent = Max(out.maxPsnSent, pkt1.psn);
43    toSend.add(pkt1, out.port);
44    out.resend.set(TIMEOUT);
45 FORWARD:
46 for (pkt', port) ∈ toSend do Forward(pkt', port);

```

packets, and return the result directly when data packet retransmission happens; but this change consequently requires the upward data packet workflow to check whether the broadcast buffer has the result ready to send, which is workable but with a bit more complexity.

Algorithm 3: Algorithm and control flow of Mode-III (continued, changes highlighted)

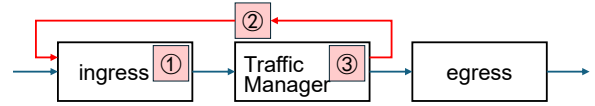
```

1 Function ReceiveAck(pkt, ep):
2   ep.lastAcked = Max(ep.lastAcked, pkt.psn);
3   ep.resend.set( ep.maxPsnSent > ep.lastAcked ? TIMEOUT : 0 );
4 Function SendAck(pkt, ep):
5   pkt' = MakePacket(ep.ip, ep.remote.ip, ep.remote.qp, ep.epsn-1,
6     ep.epsn-1 == pkt.psn ? ACK : NAK);
7   return (pkt', ep.port)
8 Function Retransmission(timer, ep, ctx):
9   for idx ∈ [ep.lastAcked + 1, ep.maxPsnSent] do
10    if ep.fromPipe.degree[idx % ctx.N] != fanin then
11      continue;
12    pkt = MakePacket(ep.ip, ep.remote.ip, ep.remote.qp, idx,
13      ep.fromPipe.payload[idx % ctx.N]);
14    Forward(pkt); timer.set(TIMEOUT);

```

For another example, in Mode-II, if RoCE applies Go-back-N (GBN) in retransmission, the switch can also maintain an epsn state (expected PSN) to optimize traffic; it filters all packets out-of-order to reduce network traffic (because out-of-order packets are dropped and retransmitted by NIC). The design space is large, and there could also be pitfalls (§5.1).

E SWITCH MICROARCHITECTURE

**Figure 17:** EPIC in switch micro architecture

Modern high-performance switches typically utilize a pipelined architecture comprising an Ingress Pipeline, a Traffic Manager (TM), and an Egress Pipeline. The Ingress Pipeline performs packet parsing and forwarding decisions, while the TM serves as the data plane core, managing on-chip shared memory for buffering and scheduling. The Egress Pipeline completes the process with packet rewriting and encapsulation. Within this framework, the IncEngine can be integrated through three distinct architectural patterns: Ingress, Loopback, or Bypass.

Ingress Integration (①) embeds the IncEngine logic directly into the ingress stages, allowing computation and modification to occur before packets reach the TM. This approach, exemplified by programmable targets like Tofino, enables line-rate processing with minimal latency. However, it is fundamentally constrained by pipeline resources, such as limited ALU stages, and frequently requires packet recirculation to handle large payloads, which can significantly consume internal switching bandwidth.

Alternatively, Loopback Integration (②) treats the IncEngine as a "look-aside" accelerator attached to a dedicated loopback

port. Packets identified by the Ingress Pipeline are routed to this port for processing before being re-submitted to the ingress stage [72]. While this mode offers high compatibility and supports complex operations without modifying the core TM logic, it inevitably increases latency due to multiple pipeline passes and places additional strain on internal switching capacity.

Finally, Bypass Integration (3) positions the IncEngine as an auxiliary component connected directly to the on-chip shared memory via a dedicated interface. In this configuration, the Ingress Pipeline tags INC packets, triggering the TM to notify the engine to aggregate data directly from memory and write results back. This design balances latency and complexity by avoiding repetitive pipeline traversals and leveraging shared memory bandwidth for high-throughput aggregation, aligning with advanced designs like Roar.

F ANALYSIS OF MODES

F.1 Transmission Efficiency

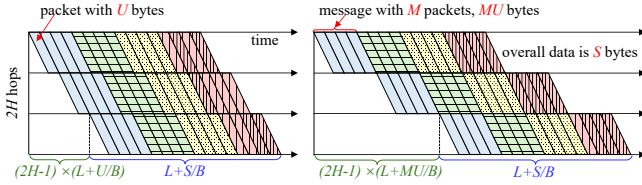


Figure 18: Transmission Efficiency

Switches operate in Store-and-Forward model but at different granularities across modes. Following the definitions in Table 2, Mode-I switches operate with a message granularity (M MTUs), requiring the reception of a full message before processing. In contrast, Mode-II/III operate with a packet (MTU) granularity (Figure 18).

Assuming an AllReduce operation traverses a tree of depth H where the path length is $2H - 1$ hops. The total time to transmit application data size S is composed of propagation delay and transmission delay: In Mode-I, the total time includes $(2H - 2)$ -hop propagation delay plus $(2H - 2)$ -hop of store-and-forward delay (message length $M \times U$) plus the final transmission time:

$$T_{Mode-I} = (2H - 2)L + (2H - 1)MU/B + S/B \quad (1)$$

In Mode-II/III, due to packet-level pipelining, the delay is dominated by the single packet serialization time:

$$T_{Mode-II/III} = (2H - 2)L + (2H - 1)U/B + S/B \quad (2)$$

Mode-II/III always outperforms Mode-I by $(2H - 1)(M - 1)U/B$ less time. In practice, if $S \gg MU$ (very large message) or $L \gg S/B$ (very small message), this advantage is not significant.

F.2 Logic Complexity

Comparing the number of modules and lines of code in implementation, the order of modes from simple to complex is Mode-II, Mode-III, and Mode-I.

F.3 Space Complexity

Mode-I uses hop-by-hop flow control, requiring buffers for one-hop bandwidth-delay product (BDP) ($2BL$). For aggregation with degree D , it needs $D - 1$ receive buffers, 1 aggregation buffer, and 1 broadcast buffer. Total $\approx (D + 1) \times 2BL$.

Mode-II relies on end-to-end flow control, requiring buffers to cover the path BDP ($2 \times (2H - 2)BL$). Total usage is $4(H - 1)BL$. Supporting reproducibility needs separate buffer for data packets, increasing the space to $4(H - 1)(D + 1)BL$.

Mode-III introduces hop-by-hop reliability, buffering for single-hop BDP ($2BL$). Total usage is $4BL$ for aggregate and broadcast. With reproducibility, it becomes $(D + 1) \times 2BL$.

The order of space overhead from small to large is Mode-III = Mode-I < Mode-II. Mode-I forces reproducibility, but Mode-III provides non-reproducibility options which achieve a smaller space.

F.4 Loss Tolerance

Let $1 - r$ denote the packet loss rate, i.e., r is the packet success rate. Endpoint throughput achieves bandwidth saturation with $r = 1$, and the throughput decreases by a factor of $F(r)$ with $r < 1$. We consider the AllReduce on a depth- H IncTree, there are $2H - 1$ hops.

We first model the impact of packet loss on throughput in AllReduce. Let r be the transmission success rate ($1 - r$ is loss rate) and $F(r)$ be the throughput decay factor.

With an aggregation of depth H , AllReduce data packets traverses $2H - 2$ hops; hop i to $i + 1$ is upward when $1 \leq i \leq H - 1$, and downward when $H \leq i \leq 2H - 2$.

In Mode-I/III, in aggregation and broadcast, transmissions between sibling nodes are independent due to independent loss retransmission. The parent's throughput is synchronized by the slowest child. Let T_i be the receive throughput at hop i . Thus,

$$T_i = \begin{cases} B, & \text{if } i = 1 \\ T_{i-1} \cdot \min_{j \in i.\text{children}} F(r_j), & \text{if } 2 \leq i < H \\ T_{i-1} \cdot \min_{j \in i.\text{siblings}} F(r_j), & \text{if } i \geq H. \end{cases}$$

In Mode-II, in aggregation, the success of aggregating all packets with the same PSN is forced to synchronize with the slowest one; in broadcast, the ranks affected by packet loss would spare extra bandwidth to retransmit, affecting sending new packets and also slowing down other lossless ranks (due to synchronization). We model the overall throughput loss by a multiplicative model:

$$T_i = \begin{cases} B, & \text{if } i = 1 \\ T_{i-1} \cdot \prod_{j \in i.\text{children}} F(r_j), & \text{if } 2 \leq x < H \\ T_{i-1} \cdot \prod_{j \in i.\text{siblings}} F(r_j), & \text{if } x \geq H. \end{cases}$$

We simplify the model by assuming $r_j = r$ and $F(r) = r$ for further analysis ⁷. Mode-I & Mode-III achieve: $T \approx B \cdot r^{2(H-1)}$; Mode-II achieves: $T \approx B \cdot (r^{D-1})^{2(H-1)} = B \cdot r^{2(H-1)(D-1)}$.

Mode-I and Mode-III outperform Mode-II in loss tolerance. In practice, if lossless layer-2 mechanisms (PFC/CBFC) is applied where $r \approx 1$, the three modes perform similarly.

G INCMANAGER ORGANIZATION

job placement, tree placement, and resource allocation

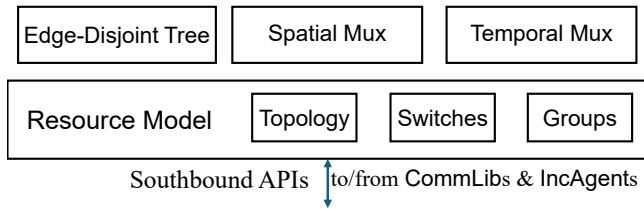


Figure 19: IncManager and policies

Figure 19 shows the organization of IncManager.

⁷In practical system, $F(r)$ could be worse than linear, because packet loss triggers congestion control, which decreases sending rate or congestion window.

H MODEL CHECKING

H.1 Implementation

Table 7: [Model Checking] LOC and Verification Time

Mode/Primitive	TLA+ LOC	Time
Mode-II/AllReduce	1222	20s
Mode-II/Reduce	1139	3s
Mode-II/Broadcast	1108	10s
Mode-III/AllReduce	1741	146min
Mode-III/Reduce	1394	9s
Mode-III/Broadcast	1386	113s

We model the IncEngine logic of Modes-II and III based TLA+ specification [38] and verify them with the TLA+ model checker (TLC). Our implementation covers three primitives—AllReduce, Reduce, and Broadcast. Table 7 summarizes the line of code (LOC) and the verification time. The code is open-sourced at GitHub⁸.

H.2 Experiment Settings

Table 8: [Model Checking] State Space Size

Mode/Primitive	Diameter	Total	Distinct
Mode-II/AllReduce	77	3981257	901703
Mode-II/Reduce	57	52105	14136
Mode-II/Broadcast	60	1763880	320128
Mode-III/AllReduce	115	2242781644	439476508
Mode-III/Reduce	65	2291727	447972
Mode-III/Broadcast	67	67902618	9911424

We evaluate model checking efficiency on a workstation with 75 cores of 2.3GHz Intel(R) Xeon(R) Silver 4316 CPU and 128 GB DRAM.

The network topology is set to be a three-level full binary tree topology (i.e., one spine switch, two leaf switch, and four clients). Each client sends three request packets. At most one packet loss may occur at any arbitrary moment. The entire state space (i.e., all possible concurrent executions) is explored.

H.3 Experiment Results

Efficiency. Table 7 and Table 8 shows the verification time and state space size of model checking. The diameter refers to the maximum distance from the initial state to all reachable states. The total number of states represents the total number of explored states, while the number of distinct states indicates the de-duplicated count.

The most time-consuming setting completes in 146 min. We regards it as acceptable, because it is a one-time cost during design, instead of runtime overhead. All other settings complete in 3 s-113 s.

Correctness. We verified our final design under different system configurations. Results show that the design guar-

antees correctness under all possible concurrent executions, even in the presence of packet loss, out-of-order, and duplication.

Since ReduceScatter and AllGather can be regarded as multiple independent Reduce and Broadcast operations, their correctness is guaranteed by this independence together with the verified correctness of Reduce and Broadcast.

The topology is small but suffices to capture bugs. Due to node symmetry and state locality, a larger topology does not provide new protocol behaviors.

H.4 Design Pitfalls

In this section, we present some representative pitfalls of our early design, discovered through model checking.

Window Synchronization. In Mode-III, hop-by-hop acknowledgments decouple the windows across different flows. Therefore, an additional synchronization mechanism must be used, as discussed in §5.1

Root-Specific Treatment. During the recursive aggregation process, the root node of the aggregation tree is special and requires dedicated handling. For example, in Mode-III, when performing AllReduce, aggregation and broadcast are decoupled in all switches but the root, which acts as a translation point of UP_DATA to DOWN_DATA. It cannot directly copy the data in AggregateData module to ReplicateData, which has the risk of overwriting an ongoing broadcast. Instead, the root should generate a local DOWN_DATA packet as if receiving from its parent, and regenerates the packet on timeout. In later design, we summarize the pipe abstraction and unify the workflow §4.4.

NAK Necessity and Rate Limiting. In Mode-III, the NAK mechanism is strongly suggested to be enabled; otherwise, a single packet loss can stall the entire aggregation tree and trigger timeout-based retransmission in every node, degrading system performance.

However, one packet loss could cause all subsequent packets to trigger NAKs, leading to redundant retransmissions. Given the limited processing capability of switches, we adopt the simplest implementation: maintaining a nak_sent flag per flow. When an in-order packet is received, the flag is set to false. When an out-of-order packet is received, the switch checks this flag—if it is false, the switch replies with a NAK and sets the flag to true; otherwise, the packet is silently dropped.

⁸ <https://anonymous.4open.science/r/epic-verification-37D3>

I TESTBED EVALUATION

I.1 Implementation

We implemented the EPIC server-side library in C++ and its switch logic in P4, managed by a lightweight Python-based control plane. The P4 program was compiled and deployed on a programmable Intel Tofino switch for hardware-level execution.

When integrating EPIC CCL with PyTorch, the message buffer in EPIC are registered RDMA buffers, and the application data are in the application buffer, not in the registered buffers. Copying data between buffers is costly. We also pipeline the memory copy with the RDMA message send/receive.

As the Tofino switch only handles integer numbers, when performing collectives on floating-point numbers, we (de)quantize the number with a fixed scaling factor; if value summation overflows, the switch rounds the value to maximum integer value; by end-to-end test, such (de)quantization does not affect training accuracy. We use the same method to handle data (de)quantization as ATP [40].

Our code is publicly available.⁹

I.2 Experiment Settings

Workloads. We evaluate the collective and application performance of EPIC. The environment settings are as §7.1. For collective evaluation, we run all six collectives with message sizes ranging from 4KB to 1GB with a scaling factor of 4. For application evaluation, we run an LLM training job with tensor and data parallelism as shown in Table 15 and Table 16.

Baselines. In the collective evaluation, we compare EPIC against SwitchML, ATP, and NCCL. We evaluate two ATP configurations: in ATP 7-to-1, one GPU serves as the Parameter Server (PS) to receive in-network aggregated data and perform local aggregation before broadcasting the results; ATP 8-to-1 follows a similar logic, but the PS also transmits data to the switch, eliminating the need for local aggregation. For NCCL, we vary the MTU (1KB and 256B) and routing algorithms (Ring and Tree) to assess their impact. Note that the Tree algorithm is only supported by AllReduce; furthermore, we omit MTU and algorithm tuning for the Barrier collective as they do not affect its performance. Importantly, SwitchML and ATP only support the AllReduce collective.

For application evaluation, we utilize the same baselines, specifically using ATP 7-to-1 to represent ATP and NCCL-Ring-1KB to represent NCCL.

I.3 Collective Performance

Table 9 illustrates the performance of the all-reduce operation. For small messages, EPIC outperforms the others be-

cause its RDMA latency is lower than the DPDK latency used by SwitchML and ATP. ATP’s Parameter Server (PS) introduces additional network hops, resulting in slightly higher latency compared to SwitchML. NCCL exhibits the highest latency and lowest bandwidth due to significant server-side control overhead.

For large messages, all three in-network computing schemes demonstrate higher bandwidth than NCCL by compressing network traffic. Furthermore, EPIC’s RDMA achieves slightly higher network bandwidth utilization than DPDK. In the ATP 8-to-1 configuration, a bottleneck occurs because the PS must simultaneously transmit data to be aggregated and aggregated results to the switch; consequently, the bandwidth is halved compared to ATP 7-to-1, falling even below that of NCCL.

For other collectives (Tables 10 to 14), NCCL continues to underperform compared to EPIC for small messages due to its control latency.

For large messages, EPIC’s performance in ReduceScatter is inferior to NCCL because it does not provide traffic compression for this specific collective. However, in asymmetric communication scenarios like Reduce, EPIC outperforms NCCL by reducing the number of network hops. Regarding Broadcast and AllGather, since there is no requirement for in-network payload aggregation,

I.4 Application Performance

The application-level evaluation yields results consistent with those observed in the collective communication analysis. In-network computing schemes outperform NCCL, with EPIC specifically demonstrating superiority over SwitchML and ATP.

For Data Parallelism (DP), the performance gap is relatively small because communication accounts for a smaller fraction of the total execution time. Conversely, for Tensor Parallelism (TP), the performance differences are more pronounced due to the higher proportion of communication overhead.

I.5 Overhead

Table 17 illustrates EPIC’s switch resource utilization. As the total size of the aggregators increases, the SRAM consumption grows significantly.

⁹ <https://anonymous.4open.science/r/EPIC-D242>.

Table 9: [Testbed] AllReduce Algorithm Throughput (Gbps)

Msg. Size (B)	4K	16K	64K	256K	1M	4M	16M	64M	256M	1G
EPIC-II	5.42	16.84	41.72	59.46	60.79	62.65	64.35	61.70	66.64	65.29
SwitchML	3.85	13.10	32.73	52.34	61.56	64.39	65.14	65.37	65.37	65.38
ATP 7-to-1	1.98	7.21	21.24	41.34	54.16	58.71	59.97	60.29	60.37	60.37
ATP 8-to-1	1.92	6.47	15.93	25.07	29.27	30.54	30.88	30.96	30.96	30.94
NCCL-Ring-1KB	0.015	0.058	0.243	0.91	3.47	13.34	29.06	40.99	46.33	47.97
NCCL-Ring-256B	0.015	0.060	0.251	0.82	3.71	12.10	26.55	36.01	39.73	41.07
NCCL-Tree-1KB	0.015	0.060	0.244	0.89	3.17	11.05	24.85	31.89	33.51	34.10
NCCL-Tree-256B	0.015	0.060	0.223	0.86	3.12	10.12	21.39	27.37	29.01	29.29

Table 10: [Testbed] Reduce Algorithm Throughput (Gbps)

Msg. Size (B)	4K	16K	64K	256K	1M	4M	16M	64M	256M	1G
EPIC-II	4.19	16.58	37.17	55.56	71.63	74.39	67.70	66.28	68.38	66.68
NCCL-1KB	0.016	0.065	0.263	1.018	3.867	14.25	40.72	64.97	67.09	67.26
NCCL-256B	0.015	0.060	0.240	0.997	3.586	12.73	12.73	57.70	59.82	59.56

Table 11: [Testbed] ReduceScatter Algorithm Throughput (Gbps)

Msg. Size (B)	4K	16K	64K	256K	1M	4M	16M	64M	256M	1G
EPIC-II	3.97	15.64	39.59	62.47	61.36	74.33	66.61	71.55	67.21	66.30
NCCL-1KB	0.014	0.056	0.218	0.926	3.34	12.92	41.07	72.29	89.58	95.58
NCCL-256B	0.014	0.056	0.240	0.927	3.65	12.70	35.97	62.24	77.74	81.32

Table 12: [Testbed] Broadcast Algorithm Throughput (Gbps)

Msg. Size (B)	4K	16K	64K	256K	1M	4M	16M	64M	256M	1G
EPIC-II	4.45	16.08	41.22	72.92	86.18	89.76	90.86	92.13	88.73	88.96
NCCL-1KB	0.015	0.061	0.24	0.913	3.52	12.92	39.99	65.61	66.60	66.60
NCCL-256B	0.015	0.063	0.24	0.99	3.61	12.92	35.63	55.54	60.02	62.86

Table 13: [Testbed] AllGather Algorithm Throughput (Gbps)

Msg. Size (B)	4K	16K	64K	256K	1M	4M	16M	64M	256M	1G
EPIC-II	4.37	16.66	39.11	72.56	86.26	89.97	91.69	92.08	90.73	90.55
NCCL-1KB	0.015	0.059	0.232	0.883	3.76	13.58	39.93	70.26	89.37	95.58
NCCL-256B	0.014	0.058	0.235	0.885	3.70	12.34	37.26	62.01	74.22	80.74

Table 14: [Testbed] Barrier Throughput

Solution	Throughput (K requests/second)
EPIC-II	165
NCCL	0.458

Table 15: [Testbed] Training job iteration time (s), context_length=2k, batch_size=256, DP=8

Model	GPT-2 Large	Qwen2.5-0.5B	Llama-3.2-1B
EPIC-II	5.46	3.59	7.18
SwitchML	5.48	3.61	7.22
ATP	5.51	3.62	7.24
NCCL	5.53	3.64	7.28

Table 16: [Testbed] Training job iteration time (s), context_length=2k, batch_size=256, TP=8

Model	GPT-2 Large	Qwen2.5-0.5B	Llama-3.2-1B
EPIC-II	21.79	13.10	21.63
SwitchML	24.33	14.58	23.88
ATP	26.62	15.92	25.93
NCCL	29.35	17.51	28.35

Table 17: [Testbed] Tofino Resource Usage

SRAM	128KB	512KB	2MB	8MB
Hash Bit	5.65%	6.05%	6.45%	6.85%
Gateway	22.92%	22.92%	22.92%	22.92%
SRAM	7.92%	7.92%	11.25%	31.67%
TCAM	1.39%	1.39%	1.39%	1.39%
VLIW Instr	8.59%	8.59%	8.59%	8.59%
Map RAM	12.33%	12.33%	17.88%	51.91%
Meter ALU	72.92%	72.92%	72.92%	72.92%
PHV	34.80%	34.80%	34.80%	34.80%

J EMULATION

J.1 Implementation

We implement six collective communication primitives (ALLREDUCE, REDUCE, BROADCAST, BARRIER, REDUCESCATTER, and ALLGATHER) across three EPIC modes on a virtual-machine testbed using `libibverbs` [48] and `libpcap` [68], demonstrating the interoperability between EPIC and RDMA verbs.

EPIC-I. In Mode 1, the switch establishes native RDMA Queue Pair (QP) connections via the `libibverbs` API and performs aggregation at the message level upon receiving complete RDMA messages. The RDMA transport layer handles all reliability semantics natively, eliminating the need for custom PSN tracking or ACK generation. The switch application layer maintains a set of aggregation slots, which are reused through modular indexing. Control information is conveyed via the 32-bit Immediate Data field encoded as `[slot_id:20][primitive:2][op:2][sender:4][root:4]`. The switch routes messages according to its role (LEAF or ROOT) and the primitive type: a LEAF switch aggregates data from its local hosts before forwarding to the parent switch, while the ROOT switch aggregates contributions from all child switches and broadcasts the result back down the tree.

EPIC-II. In Mode 2, the switch operates as a *transparent middlebox*, intercepting RoCEv2 packets via `libpcap`, performing payload aggregation and header rewriting before forwarding, without terminating the RDMA connection. The host RDMA stack retains full responsibility for reliability. The switch maintains a simplified global context (without retransmission timers). The core state array is indexed by `PSN mod SWITCH_ARRAY_LENGTH`, and a 32-bit `arrival_state` bitmap tracks the arrival status of each connection. The I/O framework in Mode 2 is built upon a single-threaded event loop using Linux `epoll`. Each physical network interface is assigned a `pcap` handle (configured in promiscuous mode, non-blocking, with a 256 MB kernel buffer) and registered with `epoll`. The main loop processes up to 256 packets per device per iteration, mapping source IPs to connection IDs before dispatching to a P4-style three-stage pipeline: *parser* (extracting ETH/IP/UDP/BTH headers) → *match* (determining direction and PSN window membership) → *action* (primitive-specific logic).

EPIC-III. In Mode 3, the switch **terminates RDMA connections**—from the host’s perspective, the switch acts as a full RoCEv2 endpoint. It intercepts raw Ethernet frames via `libpcap`, parses the complete RoCEv2 protocol stack (ETH → IPv4 → UDP → BTH → Payload → ICRC), performs aggregation at per-PSN granularity, and constructs new packets for downstream broadcast. The switch manages its own PSN space, generates ACK/NAK responses, and implements timeout-based retransmission.

Baseline. In addition to the three modes described above, we deploy OpenMPI 4.1.5 [15] in the same environment as two baselines. *MPI* routes traffic through a simple L3 forwarding switch (`soft_switch`) that relays IP packets between subnets via `libpcap` without any payload inspection or modification. *MPI-ICRC* uses the same L3 switch but additionally recomputes the RoCEv2 Invariant CRC (ICRC) on every forwarded packet, matching the per-packet ICRC overhead incurred by Mode 2 and Mode 3 when they rewrite packet headers. Comparing MPI and MPI-ICRC isolates the cost of software ICRC recomputation from the cost of in-network aggregation.

Code. Our emulation source code is publicly available.¹⁰

J.2 Experiment Settings

All three modes are evaluated on the same 1-2-4 fat-tree topology, deployed across eight OpenStack [57] virtual machines interconnected by an OVS virtual network. RDMA transport uses Soft-RoCE [47] (the `rdma_rxe` kernel module). Message sizes increase by a factor of four, covering both small and large transfers; the payload per packet is 4KB. The sliding window, aggregation slot size, and CQ size are all configured large enough to avoid performance bottlenecks. Each experiment is run 10 times, and we report the average throughput. The startup order is: Spine (ROOT) → Leaf 1 → Leaf 2 → four hosts in parallel.

J.3 Development Workload

Table 18 summarizes the code volume reported in the three mode documents. Mode 2 and Mode 3 share the same host API and controller codebase; therefore, their totals are not additive. Specifically, Mode 3 reuses 4,630 lines from Mode 2—including the INCCCL host library, protocol utilities, and the controller communication module—accounting for approximately 61% of Mode 2’s total codebase.

J.4 Performance

AllReduce (Table 19). Mode 1 achieves the highest throughput among the three modes, reaching 427 Mbps at 1 GB—roughly 4× that of Mode 2 and Mode 3. This advantage stems from message-level aggregation (64 KB per RDMA message), which reduces the number of switch-side operations by up to 64× compared with the per-packet modes. Mode 2 and Mode 3 saturate near 75 Mbps and 95 Mbps respectively once the message size exceeds 256 KB, reflecting the per-packet processing overhead of `libpcap`-based interception. Mode 3 slightly outperforms Mode 2 because its connection-termination design enables independent PSN management and avoids head-of-line blocking from the host retransmission timer. All three modes surpass MPI for small messages (≤ 64 KB), where the fixed cost of MPI’s multi-hop

¹⁰ https://anonymous.4open.science/r/EPIC_Emulation-0138/

Table 18: Development Workload

Mode	Switch code	Host/shared	Tests	Scripts	Total / Notes
EPIC-I	3,244	510	458	1,909	6,142 (includes build files)
EPIC-II	3,660	–	–	–	3,660 (switch only)
EPIC-III	2,898	3,944	583	–	7,400 (includes shared host API)

Table 19: [Emulation] AllReduce Algorithm Throughput (Mbps)

Msg. Size (B)	4K	16K	64K	256K	1M	4M	16M	64M	256M	1G
EPIC-I	2.47	10.24	35.89	78.97	182.44	247.87	381.91	417.60	425.77	426.94
EPIC-II	14.74	48.10	67.32	85.11	88.96	93.74	86.64	89.33	94.11	97.86
EPIC-III	15.69	64.14	88.69	86.77	72.54	75.54	74.86	75.46	75.13	75.64
MPI	1.71	3.72	14.89	21.12	73.90	181.22	316.46	249.17	434.01	501.59
MPI-ICRC	1.71	4.97	19.86	18.95	75.73	163.95	235.53	264.85	314.91	389.61

ring or recursive-doubling algorithm dominates; MPI catches up at large sizes owing to its optimized pipelining, ultimately reaching 502 Mbps at 1 GB.

Reduce (Table 20). Mode 1 again leads, peaking at 512 Mbps and sustaining 506 Mbps at 1 GB. The unidirectional nature of Reduce (no broadcast phase) allows Mode 1 to approach the raw RDMA link rate. Mode 2 and Mode 3 plateau around 110 Mbps and 95 Mbps respectively, consistent with the per-packet processing ceiling observed in AllReduce. MPI Reduce throughput grows steadily with message size, reaching 455 Mbps at 1 GB, but remains below Mode 1 across all sizes.

ReduceScatter (Table 21). Mode 2 and Mode 3 achieve comparable peak throughput (~105 Mbps and ~120 Mbps), while Mode 1 plateaus at ~72 Mbps. Mode 1’s lower throughput is attributable to its simulation strategy: ReduceScatter is decomposed into N sequential Reduce calls (one per rank), incurring $N \times$ the connection setup and synchronization overhead. MPI ReduceScatter scales to 601 Mbps at 1 GB, benefiting from its native implementation that overlaps reduction and data redistribution in a single pass.

Broadcast (Table 22). Broadcast exhibits a different ranking: Mode 3 achieves the highest peak at 381 Mbps (256 KB) and sustains ~200 Mbps for large messages. This is because Broadcast involves no aggregation—the switch simply replicates packets—and Mode 3’s connection termination allows it to drive downstream links at full speed without waiting for end-to-end ACKs. Mode 2 sustains ~140 Mbps, while Mode 1 plateaus near 80 Mbps, limited by the overhead of posting individual RDMA Send operations for each 4 KB chunk across multiple QP connections. MPI Broadcast scales well beyond 1 Gbps at 64 MB due to its tree-based pipelining, significantly outperforming all three INC modes for large transfers.

Mode 1 achieves the highest INC throughput at 313 Mbps (1 GB), followed by Mode 2 at 263 Mbps. Mode 3 exhibits anomalously low throughput (169 Mbps at 1 GB, and below 1 Mbps for messages ≤ 16 KB), suggesting a performance bottleneck in its broadcast-based AllGather path—likely caused by serialized per-rank broadcast rounds combined with per-packet ACK generation overhead. MPI AllGather reaches

827 Mbps at 1 GB, again benefiting from its native ring-based algorithm that pipelines data transfers across all ranks simultaneously.

Barrier (Table 30). Mode 3 delivers the highest barrier throughput at 2,502 requests/second, followed by Mode 1 at 1,331 requests/second and Mode 2 at 590 requests/second. All three modes outperform MPI (38 requests/second) by 15–66 \times , demonstrating the latency advantage of in-network synchronization: a single switch-hop round trip replaces the $O(\log N)$ steps required by MPI’s tree-based barrier. Mode 3 leads because its packet-level operation avoids the QP setup and message-framing overhead of Mode 1, while its connection termination eliminates the retransmission-timer delays that slow Mode 2.

Mode-I and MPI outperform Mode-II/III at large message sizes. The throughput ceiling of Mode 2 and Mode 3 (typically 75–140 Mbps for aggregation-based primitives) is fundamentally limited by the libpcap user-space packet processing path. Every RoCEv2 packet traverses the kernel capture buffer, crosses the kernel–user boundary, and is parsed, aggregated, header-rewritten, ICRC-recomputed, and re-injected—all in software. With a per-packet payload of only 1,024 bytes (Soft-RoCE active MTU), a 1 GB transfer generates over one million packets per connection, and the switch must process each one individually. This per-packet overhead establishes a hard throughput ceiling that cannot be overcome by increasing the message size.

Mode 1 bypasses this bottleneck entirely by operating at the *message* level. The switch establishes native RDMA QP connections and receives complete 64 KB messages via the kernel RDMA stack, reducing the number of switch-side operations by 64 \times compared with Mode 2/3. Aggregation is performed on whole messages rather than individual packets, and the RDMA transport layer handles segmentation, reassembly, and reliability transparently. As a result, Mode 1 scales to 427 Mbps (AllReduce) and 512 Mbps (Reduce) at 1 GB, approaching the effective Soft-RoCE link capacity.

MPI achieves high throughput for large messages through a different mechanism: *algorithmic pipelining*. Rather than re-

Table 20: [Emulation] Reduce Algorithm Throughput (Mbps)

Msg. Size (B)	4K	16K	64K	256K	1M	4M	16M	64M	256M	1G
EPIC-I	4.49	25.29	88.78	108.50	210.33	449.22	511.03	504.83	511.96	506.10
EPIC-II	19.02	66.77	103.23	112.01	98.91	98.82	96.11	97.17	95.25	93.96
EPIC-III	18.65	49.05	82.01	105.59	105.75	107.95	110.28	112.99	107.59	110.28
MPI	9.70	37.94	14.90	30.29	51.77	184.31	328.64	311.63	343.51	454.53
MPI-ICRC	9.49	34.39	19.74	28.65	80.84	148.66	253.76	282.72	306.78	326.42

Table 21: [Emulation] ReduceScatter Algorithm Throughput (Mbps)

Msg. Size (B)	4K	16K	64K	256K	1M	4M	16M	64M	256M	1G
EPIC-I	3.27	9.69	19.64	62.09	71.67	72.54	70.88	70.66	70.10	68.47
EPIC-II	6.55	21.84	65.53	104.85	104.85	101.68	96.55	95.69	95.35	70.20
EPIC-III	6.48	24.63	57.72	98.65	95.06	116.64	120.05	121.37	118.08	120.32
MPI	1.71	6.83	5.28	17.37	73.54	181.02	345.97	436.25	464.15	601.30
MPI-ICRC	1.70	8.69	5.28	19.83	78.24	127.33	163.14	206.49	243.26	262.97

Table 22: [Emulation] Broadcast Algorithm Throughput (Mbps)

Msg. Size (B)	4K	16K	64K	256K	1M	4M	16M	64M	256M	1G
EPIC-I	35.23	14.17	50.57	75.10	78.75	81.84	81.92	90.75	78.53	76.33
EPIC-II	25.23	62.27	117.95	115.80	125.39	139.29	145.74	132.86	142.72	138.55
EPIC-III	48.30	165.46	324.95	381.13	230.07	210.80	209.80	188.76	188.09	223.44
MPI	9.55	36.47	14.89	58.17	222.20	599.20	902.72	1212.81	832.36	984.33
MPI-ICRC	9.71	38.63	19.80	44.65	239.01	425.39	573.81	583.87	661.86	800.26

Table 23: [Emulation] AllGather Algorithm Throughput (Mbps)

Msg. Size (B)	4K	16K	64K	256K	1M	4M	16M	64M	256M	1G
EPIC-I	32.66	119.70	92.34	181.59	281.61	302.07	316.87	322.67	308.44	313.16
EPIC-II	6.35	24.40	75.88	147.62	200.50	216.69	265.47	276.48	272.88	262.54
EPIC-III	0.01	0.04	0.18	0.71	2.84	10.87	37.18	95.66	146.18	169.30
MPI	6.83	27.32	33.57	107.00	194.20	384.41	429.84	585.25	566.77	826.64
MPI-ICRC	6.83	28.15	34.35	122.71	174.96	263.41	271.78	351.22	391.54	419.66

Table 24: [Emulation] Barrier Throughput

Solution	Throughput (requests/second)
EPIC-I	1331.25
EPIC-II	590.00
EPIC-III	2502.15
MPI	37.81
MPI-ICRC	37.88

lying on in-network aggregation, MPI decomposes collective operations into multiple point-to-point transfers arranged in optimized topologies (ring, recursive doubling, or binomial tree). These algorithms overlap communication and computation across pipeline stages, allowing multiple segments to be in flight simultaneously. For Broadcast, MPI’s binomial-tree pipeline achieves over 1 Gbps by saturating all links in parallel, far exceeding the single-switch fan-out capacity of the INC modes. However, this pipelining advantage diminishes for small messages (≤ 64 KB), where the $O(\log N)$ startup latency of multi-hop algorithms dominates—precisely the regime where single-hop in-network aggregation excels.

K PACKET-LEVEL SIMULATION

K.1 Implementation

We implement a packet-level simulator based on ns-3 (version 3.43) to evaluate the performance of EPIC-II, EPIC-III, and Ring across six collective communication primitives: AllReduce, Reduce, ReduceScatter, Broadcast, AllGather, and Barrier. The code is publicly available.¹¹

K.2 Experiment Setting

For EPIC-II and EPIC-III, we use a star topology with 8 ranks connected to a single switch. For Ring, 8 ranks form a ring topology. Each link has 100 Gbps bandwidth and 1 μ s latency. We evaluate message sizes ranging from 4KB to 1GB. We vary packet loss rate from 0% to 15% on a single link, and the number of lossy links from 0 to 8 with fixed 5% loss rate per link.

K.3 Collective Performance

The performance difference between EPIC and Ring stems from two factors: *theoretical bandwidth efficiency* at large messages and *hop count* at small messages. Let N denote message size, B link bandwidth, and K the number of ranks. Since throughput is inversely proportional to completion time, we analyze performance through theoretical completion time.

Large messages: theoretical completion time matters. At large message sizes where bandwidth dominates, performance is determined by the theoretical completion time. For AllReduce, EPIC completes in N/B while Ring requires $2(K-1)N/(KB)$, resulting in EPIC achieving 1.8 \times higher throughput (89.9 vs 48.8 Gbps at 1GB). For other collectives (Reduce, Broadcast, ReduceScatter, AllGather), the theoretical gap is smaller or absent—Ring’s $(K-1)N/(KB)$ versus EPIC’s N/B for scatter/gather operations, and identical N/B for Reduce and Broadcast. Consequently, all approaches converge to near line-rate (91 Gbps) at 1GB for these collectives.

Small messages: hop count matters. At small message sizes where latency dominates, EPIC’s single-hop communication through the switch consistently outperforms Ring’s $O(K)$ hops. This advantage is most pronounced at 4KB messages, where EPIC achieves 6–10 \times higher throughput than Ring across all collectives. The gap narrows at medium sizes as pipelining effects begin to benefit Ring.

EPIC-III vs EPIC-II. EPIC-III achieves marginally higher throughput than EPIC-II in AllReduce due to its decoupled aggregation-broadcast design, which enables better pipelining. For Barrier, EPIC-III reaches 3.33×10^5 req/s versus EPIC-II’s 2×10^5 req/s.

K.4 Loss Tolerance

We evaluate EPIC-II and EPIC-III under packet loss by measuring AllReduce throughput. To isolate the retransmission

mechanism’s impact, we disable congestion control (i.e., the sending window does not shrink upon packet loss), focusing purely on how each design handles retransmissions.

As shown in Table 31, EPIC-III consistently outperforms EPIC-II across all loss rates. At 5% loss rate, EPIC-III achieves 84.9 Gbps versus EPIC-II’s 79.5 Gbps. The gap widens significantly at higher loss rates: at 15% loss, EPIC-III maintains 77.7 Gbps while EPIC-II drops to only 39.0 Gbps. Table 32 shows similar trends when varying the number of lossy links: with all 8 links experiencing 5% loss, EPIC-III achieves 72.3 Gbps versus EPIC-II’s 52.5 Gbps. The performance gap stems from different retransmission mechanisms. In EPIC-II, retransmissions are initiated by ranks upon timeout, requiring a full round-trip delay before recovery. In EPIC-III, the switch actively detects missing packets and sends NAKs to trigger immediate retransmission. Furthermore, EPIC-III’s decoupled aggregation-broadcast design prevents completed aggregations from being blocked by ongoing retransmissions, reducing head-of-line blocking effects.

K.5 Large Model Training Performance

We run SimAI to simulate large model training, with EPIC-ns3 as the backend. Model settings are shown in Table 33. Table 34 shows the model training iteration time.

EPIC-II accelerates GPT-3-175B, GPT-3-13B, Llama-65B, and Llama-7B by 2.5%, 17.7%, 12.4%, and 10.2%, respectively. In most cases, the performance gain is significant (up to 17.7%); even in the case where the gain is 2.5%, the absolute reduction of JCT is still considerable considering the scale.

¹¹ <https://anonymous.4open.science/r/EPIC-PktSim-8532>

Table 25: [Packet Simulation] AllReduce Algorithm Throughput (Gbps)

Msg. Size (B)	4K	16K	64K	256K	1M	4M	64M	256M	1G
EPIC-II	6.10	20.35	48.83	75.12	84.92	87.54	88.25	88.28	88.30
EPIC-III	10.17	30.52	61.04	81.38	88.78	89.03	89.90	89.92	89.92
Ring	1.02	3.81	12.21	27.90	41.12	46.64	48.66	48.76	48.79

Table 26: [Packet Simulation] Reduce Algorithm Throughput (Gbps)

Msg. Size (B)	4K	16K	64K	256K	1M	4M	64M	256M	1G
EPIC-II	10.17	30.52	61.04	81.38	88.78	90.84	91.46	91.49	91.50
EPIC-III	10.17	30.52	61.04	81.38	88.78	90.84	91.46	91.49	91.50
Ring	1.80	5.09	9.39	19.53	47.64	74.40	90.19	91.16	91.41

Table 27: [Packet Simulation] ReduceScatter Algorithm Throughput (Gbps)

Msg. Size (B)	4K	16K	64K	256K	1M	4M	64M	256M	1G
EPIC-II	10.17	30.52	61.04	81.38	88.78	90.84	91.46	91.49	91.50
EPIC-III	10.17	30.52	61.04	81.38	88.78	90.84	91.46	91.49	91.50
Ring	1.91	7.12	23.74	53.41	77.68	87.64	91.24	91.43	91.48

Table 28: [Packet Simulation] Broadcast Algorithm Throughput (Gbps)

Msg. Size (B)	4K	16K	64K	256K	1M	4M	64M	256M	1G
EPIC-II	10.17	30.52	61.04	81.38	88.78	90.84	91.46	91.49	91.50
EPIC-III	10.17	30.52	61.04	81.38	88.78	90.84	91.46	91.49	91.50
Ring	2.77	6.78	10.61	20.78	49.45	75.48	90.29	91.19	91.41

Table 29: [Packet Simulation] AllGather Algorithm Throughput (Gbps)

Msg. Size (B)	4K	16K	64K	256K	1M	4M	64M	256M	1G
EPIC-II	6.98	22.71	52.08	76.59	87.29	90.42	91.43	91.48	91.49
EPIC-III	7.18	23.25	52.79	76.97	87.41	90.45	91.43	91.48	91.49
Ring	13.35	37.15	67.02	83.88	89.50	90.99	91.47	91.49	91.50

Table 30: [Packet Simulation] Barrier Throughput

Solution	Throughput (requests/second)
EPIC-II	2E5
EPIC-III	3.33E5
ToRank0	1.42E5

Table 31: [Packet Simulation] Throughput vs Loss Rate

Loss(%)	0	0.1	0.5	1	2	5	8	10	12	15
EPIC-II	87.54	86.33	86.81	86.09	84.46	79.52	75.48	73.01	47.17	39.01
EPIC-III	89.03	88.53	88.53	88.28	87.54	84.92	82.67	81.17	79.72	77.74

Table 32: [Packet Simulation] Throughput (Gbps) vs Lossy Links (5% loss)

Links	0	1	2	3	4	5	6	7	8
EPIC-II	87.54	79.52	74.05	70.07	64.97	63.78	59.07	55.31	52.52
EPIC-III	89.03	84.92	82.02	79.31	77.54	76.78	75.67	74.94	72.34

Table 33: [SimAI/NS3 Simulation] Large Model Settings

Settings	GPU Flops	num layers	hidden size	num parameters	num tokens per_seq	batch size	dtype size	TP, DP, PP
GPT-3 175B	125e12	96	12288	175e9	2048	1536	16	4,32,8
GPT-3 13B	312T	40	5120	13B	2048	128	2bytes	8,16,1
Llama-65B	312T	80	8192	65B	4096	128	2bytes	8,16,1
Llama-7B	312T	32	4096	6.7B	4096	128	2bytes	8,16,1

EPIC

Table 34: [SimAI/NS3 Simulation] Model Training Iteration Time

Model	GPT-3-175B	GPT-3-13B	Llama3-65B	Llama3-7B
EPIC-II	32.35s	1.154s	8.831s	1.132s
EPIC-III	32.37s	1.159s	8.856s	1.134s
Ring	33.19s	1.403s	10.08s	1.261s

Table 35: [Packet Simulation, Mode-III] AllReduce Algorithm Goodput (Gbps), with/without switch replying CNP

Msg. Size (B)	1K	16K	16K	256K	1M	4M	16M	64M
Switch Not Replying CNP	13.96	38.66	70.37	88.09	94.38	95.99	95.87	90.45
Switch Replying CNP	13.96	38.66	70.37	88.09	94.38	44.60	43.32	20.25

L FLOW-LEVEL SIMULATION

L.1 Implementation

Simulator. The implementation of the flow-level simulator used in this section is publicly available in an anonymized repository.¹² The simulator is implemented in C++ based on OMNeT++ [56], and consists of approximately 3.9K lines of code.

We implement a custom flow-level simulator based on OMNeT++, designed to model single-tenant and multi-tenant large-scale distributed training workloads over a fat-tree interconnect, with explicit support for different in-network compute (INC) resource allocation policies. The simulator operates at the granularity of communication groups (i.e., collective operations), rather than packets, which enables scalable evaluation of job-level performance metrics such as job completion time (JCT) under realistic cluster scales.

The simulator explicitly models both rank behaviors and network behaviors. In each simulation step, ranks alternate between computation and communication phases, while the network allocates bandwidth and INC resources subject to link capacity and switch-level constraints. During communication, the network applies a waterfilling-based algorithm to estimate per-group throughput and advances data transmission accordingly.

Each job consists of multiple iterations, and each iteration triggers a fixed set of communication groups. INC resource allocation decisions are made independently for each communication group based on the selected execution mode and

current resource availability.

We model a three-tier fat-tree topology consisting of leaf, spine, and core switches. Each switch has 32 ports, and each link has a bandwidth capacity of 100 Gbps. Communication groups are mapped onto aggregation trees spanning the fat-tree topology. Switches are associated with a limited amount of INC-related resources, abstracted differently by each INC policy.

We consider two server-side configurations depending on the network fabric. In the pure fat-tree setting, each GPU is modeled as an independent endpoint connected to the network, corresponding to a server equipped with a single GPU and a dedicated network interface (or equivalently, a multi-GPU server with one network interface per GPU). In the fat-tree with ScaleUp setting, multiple GPUs are co-located within the same server. Intra-server communication among these GPUs is handled by the ScaleUp fabric and does not consume fat-tree network bandwidth, while inter-server communication is carried over the fat-tree network.

We evaluate the simulator under four experimental settings, formed by the Cartesian product of workload type and network fabric. Specifically, we consider single-tenant training and multi-tenant training, and for each workload type we test on both a pure fat-tree fabric and a fat-tree with ScaleUp fabric. The single-tenant setting models a training job using 128 GPUs, while the multi-tenant setting models concurrent jobs on a 2048-GPU cluster.

L.2 Experimental Settings

Baselines. We implement four execution policies and settings corresponding to different INC strategies.

In Setting 0 (Ring), all communication groups execute using conventional collective communication without in-network aggregation. Communication volumes are not reduced, and all traffic traverses the network without consuming INC resources.

In Setting 1 (EDT), we implement an edge-disjoint tree based INC policy. A communication group is granted INC if and only if none of the links on its aggregation tree are currently used by another INC-enabled group. Link usage is tracked explicitly. If any link conflict exists, the group falls back to non-INC execution. INC allocation is therefore enforced at link granularity, ensuring strict edge disjointness among concurrent INC trees.

In Setting 2 (Spatial Mux), each switch maintains a fixed number of INC resource slots. A communication group is granted INC if all switches along its aggregation tree have at least one available slot. Once allocated, INC resources are reserved for the entire lifetime of the job, and are not released until the job completes. This models static partitioning of switch INC resources across concurrent jobs.

In Setting 3 (Temporal Mux), INC allocation follows the

¹² <https://anonymous.4open.science/r/inc-flow-sim-77D5/>

same admission condition as spatial multiplexing, but resources are allocated and released dynamically at the granularity of individual communication groups. After a communication group completes, its occupied INC resources are immediately released and may be reused by other groups. This enables time-sharing of INC resources across jobs and improves overall utilization under multi-tenant contention.

For each communication group, the simulator determines whether INC is enabled according to the selected mode and current resource availability. If INC is granted, the effective communication volume is reduced accordingly; otherwise, the group executes in non-INC mode. The simulator advances until all communication groups and computation phases of a job complete, at which point the job completion time is recorded.

Topology. We adopt a three-tier fat-tree topology consisting of leaf, spine, and core switches to model communication in large-scale distributed training systems.

In the single-tenant setting, the topology is configured to support a single 128-GPU training job. Each leaf switch connects to 8 servers. A pod contains 4 leaf switches and 4 spine switches with full leaf–spine connectivity, and each spine switch connects to 4 core switches. Under this configuration, each pod interconnects $4 \times 8 = 32$ GPUs, and the system consists of 4 pods in total, providing exactly 128 GPUs. This setting exposes both intra-pod and inter-pod communication paths for a large single-tenant workload.

In the multi-tenant setting, we scale up the topology to support concurrent jobs. Each leaf switch connects to 16 servers, and each pod consists of 16 leaf switches and 16 spine switches with full leaf–spine connectivity, while each spine switch connects to 8 core switches. As a result, each pod interconnects $16 \times 16 = 256$ GPUs, and the overall system comprises 8 pods, forming a shared network fabric for multi-tenant training with increased contention at the spine and core layers.

For scale-up modeling, we bind 8 GPUs to a single server and assume that GPUs within the same server communicate via high-bandwidth, low-latency links such as NVLink. This intra-server communication does not consume fat-tree network bandwidth, whereas inter-server communication traverses the fat-tree fabric, allowing us to distinguish scale-up and scale-out communication in our simulations.

Workloads. We evaluate our design using three workload traces that differ in how job compositions and network pressures are constructed.

Trace1 is a manually configured synthetic workload that serves as a controlled baseline. In this trace, we explicitly define the job size distribution rather than deriving it from production data. We consider five representative job sizes, namely 8, 16, 32, 64, and 128 GPUs, and assign them fixed proportions of 30%, 30%, 25%, 10%, and 5% of the total jobs,

respectively. By construction, Trace1 provides a stable and interpretable workload composition, allowing us to isolate the impact of network configurations and INC strategies without interference from trace-specific artifacts.

Trace2 is derived from the Alibaba Lingjun dataset [6], which provides CSV summaries of distributed training jobs collected from a large-scale production GPU cluster. We implement a custom script to extract job sizes and their relative proportions from these summaries, and use the resulting distribution to generate synthetic workloads for simulation. Trace2 therefore reflects the job mix observed under the default production network configuration.

Trace3 is constructed by keeping the same workload composition as Trace2, while modifying the network topology to increase communication pressure. Specifically, we reduce the number of core-layer switches by half, which increases the likelihood of cross-pod communication and contention in the upper layers of the fat-tree. This trace enables us to study the behavior of different INC strategies under heightened network bottlenecks while holding the workload mix constant.

L.3 Performance

We first compare the three INC-based schemes with the conventional ring-based collective communication. Across all evaluated settings, all INC schemes consistently achieve lower job completion time (JCT) than the ring baseline, demonstrating the benefit of in-network aggregation.

We then analyze the impact of limited switch memory on JCT. When switch memory is scarce, the JCT performance ordering follows EDT, spatial multiplexing, and temporal multiplexing, with temporal multiplexing achieving the lowest JCT due to its more flexible allocation of switch resources. As switch memory becomes sufficient, the JCT gap between spatial and temporal multiplexing diminishes, and both schemes achieve comparable performance, while EDT remains inferior due to its stricter allocation constraints.

In the multi-tenant setting, temporal multiplexing may lead to slightly higher JCT for some individual jobs, as INC resources can be released during computation phases, whereas spatial multiplexing holds resources for the entire job. However, this dynamic allocation significantly improves tail JCT and results in the lowest average JCT overall by utilizing switch memory more efficiently.

Table 36: [Flow Simulation] JCT of GPT-3-175B on 128-GPU Fat-tree

Switch SRAM (Unit)	4	8	16	32
Ring	253	253	253	253
EDT	179	179	179	179
Spatial Mux	179	158	137	137
Temporal Mux	158	137	137	137

Table 37: [Flow Simulation] JCT of GPT-3-13B on 128-GPU Fat-tree

Switch SRAM (Unit)	4	8	16	32
Ring	33.55	33.55	33.55	33.55
EDT	20.66	20.66	20.66	20.66
Spatial Mux	20.66	19.10	17.54	17.54
Temporal Mux	19.10	17.54	17.54	17.54

Table 38: [Flow Simulation] JCT of Llama-65B on 128-GPU Fat-tree

Switch SRAM (Unit)	4	8	16	32
Ring	211	211	211	211
EDT	129	129	129	129
Spatial Mux	129	121	113	113
Temporal Mux	121	113	113	113

Table 39: [Flow Simulation] JCT of Llama-7B on 128-GPU Fat-tree

Switch SRAM (Unit)	4	8	16	32
Ring	37.78	37.78	37.78	37.78
EDT	21.29	21.29	21.29	21.29
Spatial Mux	21.29	20.49	19.68	19.68
Temporal Mux	20.49	19.68	19.68	19.68

Table 40: [Flow Simulation] JCT of GPT-3-175B on 128-GPU Fat-tree with Scaleup

Switch SRAM (Unit)	4	8	16	32
Ring	106	106	106	106
EDT	84.6	84.6	84.6	84.6
Spatial Mux	84.6	63.6	63.6	63.6
Temporal Mux	84.6	63.6	63.6	63.6

Table 41: [Flow Simulation] JCT of GPT-3-13B on 128-GPU Fat-tree with Scaleup

Switch SRAM (Unit)	4	8	16	32
Ring	7.94	7.94	7.94	7.94
EDT	6.38	6.38	6.38	6.38
Spatial Mux	6.38	4.82	4.82	4.82
Temporal Mux	6.38	4.82	4.82	4.82

Table 42: [Flow Simulation] JCT of Llama-65B on 128-GPU Fat-tree with Scaleup

Switch SRAM (Unit)	4	8	16	32
Ring	47.6	47.6	47.6	47.6
EDT	39.8	39.8	39.8	39.8
Spatial Mux	110.0	39.8	32.0	32.0
Temporal Mux	110.0	39.8	32.0	32.0

Table 43: [Flow Simulation] JCT of Llama-7B on 128-GPU Fat-tree with Scaleup

Switch SRAM (Unit)	4	8	16	32
Ring	5.01	5.01	5.01	5.01
EDT	4.20	4.20	4.20	4.20
Spatial Mux	4.20	3.40	3.40	3.40
Temporal Mux	4.20	3.40	3.40	3.40

Table 44: [Flow Simulation] Average JCT of Multi-tenant Jobs on 2048-GPU Fat-tree

Workloads	Trace1	Trace2	Trace3
Ring	6190	6245	6267
EDT	4108	4635	4666
Spatial Mux	3920	4722	4791
Temporal Mux	3750	4621	4618

Table 45: [Flow Simulation] 8-GPU Jobs' JCT in Trace2 on 2048-GPU Fat-tree with and without scaleup

Workload	without scaleup	with scaleup
Ring	72.0	41.9
EDT	56.0	41.1
Spatial Mux	56.2	40.9
Temporal Mux	56.0	40.9

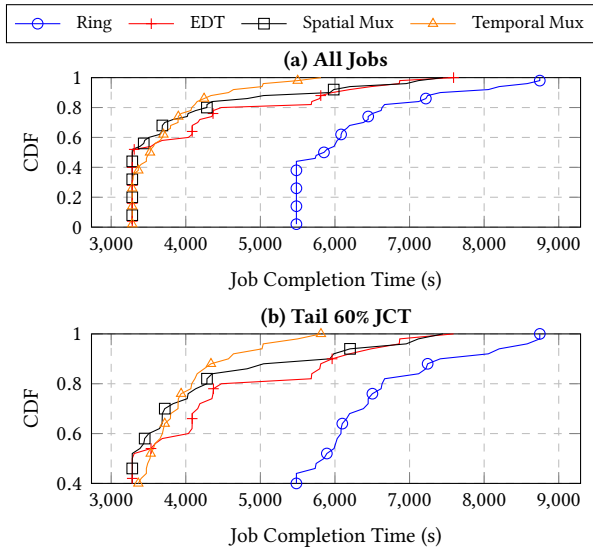


Figure 20: [Flow Simulation] JCT CDF of Trace 1 on 2048-GPU Fat-tree.

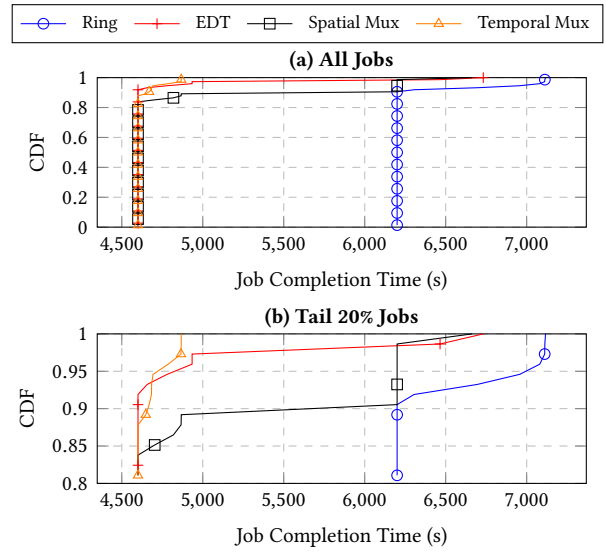


Figure 22: [Flow Simulation] JCT CDF of Trace 3 on 2048-GPU Fat-tree.

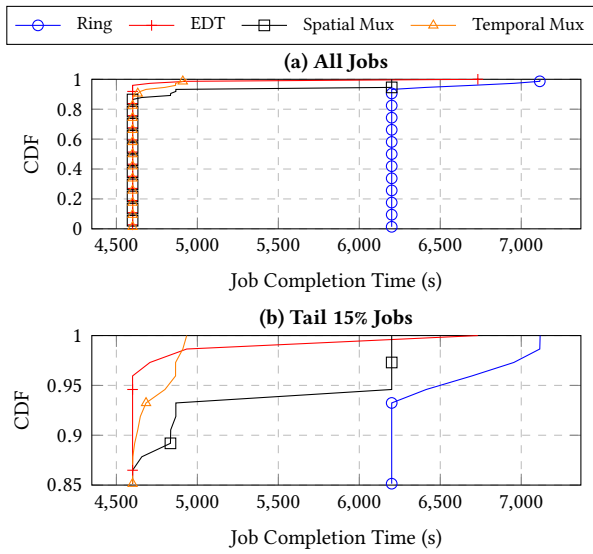


Figure 21: [Flow Simulation] JCT CDF of Trace 2 on 2048-GPU Fat-tree.

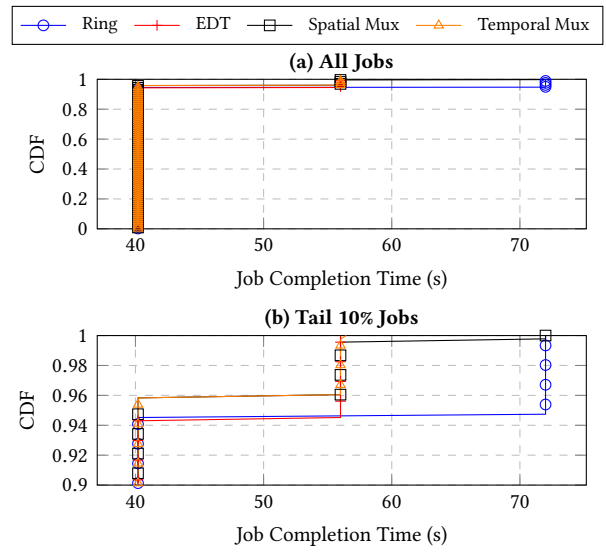


Figure 23: [Flow Simulation] 8-GPU's JCT CDF of Trace 2 on 2048-GPU with scaleup.

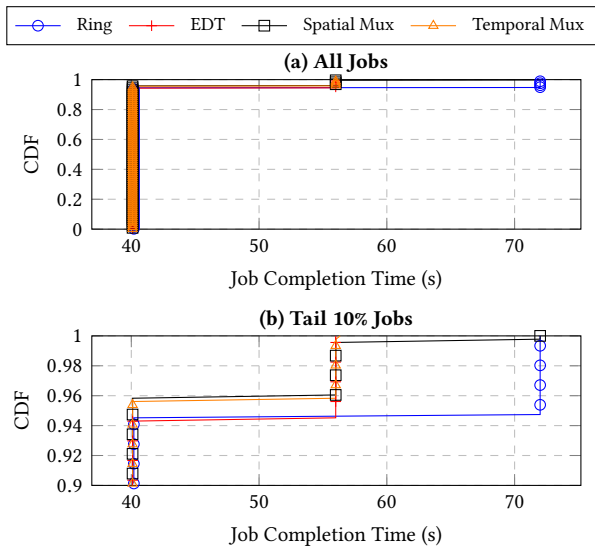


Figure 24: [Flow Simulation] 8-GPU's JCT CDF of Trace 2 on 2048-GPU with INC-improved scaleup.

M FPGA IMPLEMENTATION

M.1 Implementation from a Cluster Vendor

As EPIC Mode-II presents the lowest barrier to implementation, we collaborated with a cluster vendor to facilitate its FPGA-based realization and evaluation. The implementation was developed using Verilog on the Intel Agilex™ 7 FPGA M-Series 039 (R47A) platform.

To assess the performance of the proposed IncEngine, we conducted cycle-accurate RTL simulations focused on throughput, per-packet latency, and resource utilization. Experimental results indicate that for an 8-rank configuration, the total latency from the arrival of the final packet to the commencement of aggregated result output is approximately 230 ns. This total duration encompasses the entire processing pipeline of the parser and deparser, with the core functional latency of the aggregation engine specifically accounting for 53 ns.

The hardware resource overhead is primarily influenced by the buffer capacity and supported data types. The current design supports the FP32 data type with a default buffer specification of 8 MB, which can be configured for either 16 ranks \times 2 groups or 32 ranks \times 1 group. Under the FP32 configuration, as the buffer capacity scales from 2 MB to 16 MB, the Adaptive Logic Module (ALM) consumption ranges from 265,969 to 306,642, while memory bit utilization increases from approximately 54.5 Mb to 322.3 Mb. Across all buffer sizes, the Digital Signal Processor (DSP) utilization remains constant at 256 units (Table 46).

M.2 Implementation from an Institute

The EPIC specification was delivered to a research institute for comprehensive FPGA implementation and performance evaluation. The system is implemented on the Xilinx Virtex UltraScale+ VU13P platform, utilizing approximately 6,500 lines of Verilog code for the entire logic, with the IncEngine itself comprising 5,500 lines.

To ensure high-throughput processing, two critical FPGA-specific optimizations are integrated: first, a block-based SIMD parallel computing method is employed to divide large bit-width payloads into independent sub-vectors, thereby overcoming the bottlenecks of element-wise serial processing; second, a speculation-based consistency control mechanism is implemented to resolve read-after-write (RAW) haz-

Table 46: [FPGA, Cluster Vendor] Resource Consumption with FP32

Buffer Size (MB)	ALM	Memory Bits	DSP
2	265969	54484032	256
4	271160	92753792	256
8	287376	169571264	256
16	306642	322347776	256

ards arising from varying data path lengths between initial and retransmitted packets without stalling the pipeline.

Experimental evaluations conducted at a 250MHz clock frequency demonstrate that the system achieves line-rate 100Gbps throughput across various packet types, with end-to-end latencies for 1 KB payloads ranging from 96 ns for direct forwarding to 244 ns for FP32 upstream aggregation. Detailed resource utilization analysis shows that for a 1 MB buffer configuration, the Int32 implementation consumes 867,479 LUTs (50.20%) and 235 BRAMs (8.74%), while the FP32 configuration increases the demand to 987,308 LUTs (57.14%) and 343,724 Flip-Flops (9.95%), reflecting the increased complexity of floating-point operations. Table 47 and Table 48 shows the overall and IncEngine’s resource consumption.

N EVALUATION BY CHIP VENDOR

The EPIC specification was delivered to a prominent chip vendor for a comprehensive hardware implementation assessment. The core logic of the engine was developed using Verilog, comprising 66,377 lines of code to define the Register-Transfer Level (RTL) hardware description, which was subsequently verified through cycle-accurate SystemVerilog simulations.

Architecturally, the design prioritizes high-performance collective communications, supporting critical operations such as Broadcast, AllReduce, and ReduceScatter with internal FP32 precision to ensure numerical consistency. The design also support other data types such as FP16, BF16, INT32, but internally, all data types except INT32 are converted to FP32 for computation and converted back after computation. The design chooses the reproducible computation (buffering all data then computing).

Experimental results from the RTL simulations indicate that each packet incurs a processing latency of 50 ns, with a single engine providing a throughput of 3.2 Tbps. When integrated into the switching chip, a cluster of eight IncEngine units achieves an aggregate processing capacity of 25.6 Tbps. Each IncEngine supports 64 communication groups, each group with 16 members.

Regarding hardware overhead, the design was synthesized using a 28nm process technology. A single IncEngine instance, configured with 512 FP32 ALUs, 512 UINT ALUs and a 1 MB payload buffer, occupies an area of 4.89 mm². Consequently, the total area overhead for the eight integrated engines amounts to 39.12 mm², demonstrating a scalable and efficient footprint for high-bandwidth in-network computing. The chip specification include:

- **Collective Types:** Broadcast, AllGather, Reduce, ReduceScatter, AllReduce.
- **Operation Types:** SUM, MIN, MAX.
- **Data Types:** FP32, FP16, BF16, INT32.

Table 47: [FPGA, Institute A] Overall Resource Consumption

Data Type	Buffer Size	LUTs (1,728,000)	LUTRAM (791,040)	FF (3,456,000)	BRAM (2,688)
Int32	1MB	867479(50.20%)	637900(80.64%)	169382(4.90%)	235(8.74%)
Int32	512KB	863426(49.97%)	637900(80.64%)	165024(4.78%)	122(4.54%)
Int32	256KB	863433(49.97%)	637900(80.64%)	165026(4.78%)	122(4.54%)
Int32	128KB	468170(27.09%)	319116(40.34%)	158769(4.69%)	122(4.54%)
FP32	1MB	987308(57.14%)	638924(80.77%)	343724(9.95%)	235(8.74%)
FP32	512KB	983245(56.90%)	638924(80.77%)	339366(9.82%)	122(4.54%)
FP32	256KB	983250(56.90%)	638924(80.77%)	339369(9.82%)	122(4.54%)
FP32	128KB	588010(34.03%)	320140(40.47%)	333111(9.64%)	122(4.54%)

Table 48: [FPGA, Institute A] IncEngine Resource Consumption

Data Type	Buffer Size	LUTs (1,728,000)	LUTRAM (791,040)	FF (3,456,000)	BRAM (2,688)
Int32	1MB	866023(49.48%)	637568(80.6%)	144989(4.20%)	235(8.74%)
Int32	512KB	850970(49.25%)	637568(80.6%)	140631(4.07%)	122(4.54%)
Int32	256KB	850973(49.25%)	637568(80.6%)	140629(4.07%)	122(4.54%)
Int32	128KB	462529(26.77%)	318784(40.3%)	140583(4.07%)	122(4.54%)
FP32	1MB	974852(56.42%)	638592(80.73%)	319331(9.24%)	235(8.74%)
FP32	512KB	970789(56.18%)	638592(80.73%)	314973(9.11%)	122(4.54%)
FP32	256KB	970804(56.18%)	638592(80.73%)	314971(9.11%)	122(4.54%)
FP32	128KB	582370(33.70%)	319808(40.43%)	314971(9.11%)	122(4.54%)

- Capacity: 25.6 Tbps